UPPSALA
UNIVERSITET

IT Licentiate theses
2018-002

Ammonium Based Aeration Control in Wastewater Treatment Plants - Modelling and Controller Design

TATIANA CHISTIAKOVA

UPPSALA UNIVERSITY
Department of Information Technology

UPPSALA
UNIVERSITET

Ammonium Based Aeration Control in Wastewater Treatment Plants - Modelling and Controller Design

Tatiana Chistiakova
tatiana.chistiakova@it.uu.se

April 2018

Division of Systems and Control
Department of Information Technology
Uppsala University
Box 337
SE-751 05 Uppsala
Sweden

http://www.it.uu.se/

Dissertation for the degree of Licentiate of Philosophy in Electrical Engineering with Specialization in Automatic Control

ISSN 1404-5117
Printed by the Department of Information Technology, Uppsala University, Sweden

Abstract

Wastewater treatment involves many processes and methods which make a treatment plant a large-scaled and complex system. A fundamental challenge is how to maintain a high process efficiency while keeping the operational costs low. The variety in plant configurations, the nonlinear behaviour, the large time delays and saturations present in the system contribute to making automation and monitoring a demanding task.

The biological part of a wastewater treatment process includes an aeration of the water and this process has been shown to often result in the highest energy consumption of the plant. Oxygen supply is a fundamental part of the activated sludge process used for aerobic microorganisms growing. The concentration of the dissolved oxygen should be high enough to maintain a sufficient level of biological oxidation. However, if the concentration is too high the process efficiency is significantly reduced leading to a too high energy consumption. Hence, there are two motivations behind the aeration control task: process efficiency and economy. One of the possible strategies to adjust the dissolved oxygen level in a nitrifying activated sludge process is to use ammonium feedback measurements.

In this thesis, an activated sludge process is modelled and analysed in terms of dissolved oxygen to ammonium dynamics. First, the data obtained from a simplified Benchmark Simulation Model no.1 was used to identify the system. Both linear and nonlinear models were evaluated. A model with a Hammerstein structure where the nonlinearity was described by a Monod function was chosen for a more thorough study. Here, a feedback controller was designed to achieve $\mathcal{L}_2$-stability. The stability region was pre-computed to determine the maximum allowed time delay for the closed loop system. Finally, a feedforward controller was added to the system, and shown to significantly improve the disturbance rejection properties.

Acknowledgments

First of all, I would like to thank my supervisors Prof. Bengt Carlsson and Adj. Prof. Torbjörn Wigren for their guidance and support. Your ideas and enthusiasm helped me to start this journey. Your knowledge and efficiency are really impressive and encouraging!

I am grateful to my external supervisor, Doc. Jesús Zambrano, for his help with the knotty BSM1. Your pure interest in any research topic and willingness to share ideas are very much appreciated.

During the first year, I had a joyful time in a shared office, I would like to give thanks to my former office-mates for it and for introducing me to *fika* concept. A big thanks also goes to all former and present SysCon-ers for a pleasant ambience during and after work. My dear friends outside Sweden (i.e. academia), thank you for constantly linking me up with a real world!

Last but not least, I would like to express my sincere and biggest gratitude to my family. This whole adventure is possible only due to a support and faith of my parents who always get behind my aspirations, thank you! Jonas, thank you for your endless patience and the greatest encouragements throughout the time.

Uppsala, April 2018
Tania

Glossary and Notation

Abbreviations

WWTP	wastewater treatment plant
ASP	activated sludge process
DO	dissolved oxygen
MPC	model predictive control
PI	proportional integral
BSM1	Benchmark Simulation Model no.1
ASM1	Activated Sludge Model no.1
SISO	single-input-single-output
MISO	multiple-input-single-output
MIMO	multiple-input-multiple-output
LOE	linear output error
PEM	prediction error method
RPEM	recursive prediction error method
PRBS	pseudorandom binary sequence
RAS	return activated sludge
WAS	waste activated sludge

Notation

NH_4	ammonium

Contents

Chapter 1

Introduction

In this work, two subjects are studied: the modelling of the dissolved oxygen to ammonium dynamics and the aeration control in a nitrifying activated sludge process (ASP) of a wastewater treatment plant (WWTP). The purpose is to study how simplified dynamic models can be obtained and used to design low-order controllers with guaranteed stability properties.

This chapter provides a background to the studied field as well as a detailed motivation for the work. The contributions and publications are also described together with the outline of the thesis.

1.1 Research Motivation

Wastewater treatment has a long history. However, it has experienced a significant development in the last century due to a fast increase in population and industrial development, [15] and [39]. Wastewater treatment is a large-scale and complex process consisting of several essential parts, like mechanical, biological and chemical treatment. The focus of this work is on the biological treatment.

Biological treatment is a part of the secondary treatment when the wastewater has already been treated with filters and clarified in quiescent basins. Various organic elements and forms of nitrogen are removed during the biological treatment. One of the typical approaches for this treatment is the activated sludge process, developed in the early 1900s in the UK, [15]. In an ASP, bacteria are used for nitrification when ammonia is converted to nitrate. These bacteria (aerobes) need free dissolved oxygen (DO) for growth, [10] and [12]. The aeration of water supplies the microorganisms with the demanded concentration of DO. This process is generally the most energy consuming one in a WWTP, [2] and [9].

The DO concentration needs to be high enough to sustain the selected

nitrogen removal rate. If the DO level is too high, the result is a high cost and a low relative efficiency. Hence, optimal aeration control is of high significance for the treatment process.

A common approach for aeration control is to maintain the DO level around a fixed and given DO set-point, [30]. However, studies have shown that using ammonium feedback to control the DO set-point can decrease the energy consumption without increasing the effluent ammonium load, [1], [7] and [42]. This strategy makes use of the ammonium concentration level in, for example, the effluent flow to select a DO set-point for all controllers of aerated zones where an ASP occurs.

An ASP can be characterised as a complex, nonlinear dynamic process. This process together with multiple inputs and various disturbances require sophisticated control in order to maintain stable and high performance under different conditions. Model predictive control (MPC) is one of the approaches that is nowadays introduced in WWTPs. Studies have shown that MPC could sometimes outperform simple controllers, [28], [29] and [41]. However, MPC controllers are computationally complex with complicated stability properties which motivates the study and use of other simpler alternatives, like in [1], [2] and [8]. A natural solution for aeration control would be the use of proportional integral (PI) control due to its simplicity and, most often, sufficient performance, [3] and [17].

A suitable tuned controller for an aeration process can be achieved by estimating a model of the DO to ammonium dynamics and apply this model for controller design. A linear time-invariant model is a common starting point to perform system identification in an ASP, [20] and [37]. Still, a high order and nonlinear character of the system may make it challenging for linear models to achieve an accurate system description. Therefore, nonlinear system identification, in particularly, block oriented system modelling, [11] and [21], might be beneficial for describing input-output relationships in systems like an ASP.

1.2 Contributions

There are two contributions of this work. The first one is to perform nonlinear system identification of the DO to effluent ammonium dynamics in a nitrifying ASP. The identification is carried out on data obtained from a simplified version of the Benchmark Simulation Model no.1 (BSM1), [6]. One linear and one nonlinear system identification approach are evaluated and compared. Due to the nonlinear character of the process, Hammerstein models were applied for their simplicity. The process disturbances are taken into account and modelled along with the DO to ammonium dynamics.

The first contribution enables model based design of nonlinear feedback and feedforward controllers, which defines the second contribution. The controller design are based on methods that enforce $\mathcal{L}_2$-stability. First, a pre-computation of the $\mathcal{L}_2$-stability region of the control system is performed in order to obtain the feedback controller parameters. The Popov criterion is applied for this purpose. Another part of the controller design adds feedforward. The feedforward controller exploits the identified disturbance model and aims to predict and reject the high frequency parts of the disturbance, with the feedback controller handling the low frequency parts.

1.3 Publications

The following (reformatted) papers are appended:

Paper I

T. Chistiakova, P. Mattsson, B. Carlsson and T. Wigren. Nonlinear system identification of the dissolved oxygen to effluent ammonia dynamics in an activated sludge process. In *Proceedings of the 20th IFAC World Congress*, pp. 3917–3922, Toulouse, France, July 2017.

A simplified ASP is analysed and identified using a Hammerstein model structure with two different identification algorithms: off-line and online (recursive) prediction error methods.

Paper II

T. Chistiakova, B. Carlsson and T. Wigren. Non-linear modeling of the dissolved oxygen to ammonium dynamics in a nitrifying activated sludge process. In *Proceedings of the 12th IWA Conference on Instrumentation, Control and Automation*, pp. 85–93, Quebec City, Quebec, Canada, June 2017.

A number of identification methods are examined to find an accurate dynamic model of the DO to effluent ammonium relation in an ASP. The identification is performed on data from a simplified version of BSM1, and compares one linear model to several Hammerstein models. The Hammerstein models provide new grey-box parametrizations of the static nonlinear part of the model.

Paper III

T. Chistiakova, T. Wigren and B. Carlsson. Input-output stability based controller design for a nonlinear wastewater treatment process. To appear in *Proceedings of ACC 2018*, Milwaukee, WI, USA, June 2018.

An identified model with a Hammerstein structure is used for tuning of a leaky PI controller. The tuning uses the Popov inequality for a stability region computation. The stability region accounts for time delays caused by the process dynamics, and static nonlinear effects associated with the aeration part of the process.

Paper IV

T. Chistiakova, T. Wigren and B. Carlsson. Combined $\mathcal{L}_2$-stable feedback and feedforward aeration control in a wastewater treatment plant. *Submitted for publication*, March, 2018.

A combined feedback and feedforward controller is presented for ammonium - based aeration control. The system behaviour is predicted using disturbance measurements of the inflow. The required set point value is further regulated by a feedback controller. The design accounts for disturbance and feedback delays, as well as for the nonlinearity associated with the dissolved oxygen to ammonium dynamics. The stability based feedback design suggested in Paper III is applied.

1.4 Thesis Outline

The contents of the thesis is divided into three parts. The first part, Chapter 2, provides a general description of WWTPs and explains the ASP simulation model.

Chapter 3 gives an overview of topics in system identification, controller design, control theory and stability analysis that are relevant for the thesis. In particular, linear and nonlinear identification methods are described followed by an explanation of the feedback and feedforward control structures for WWTPs. Methods for controller design and the background for the input-output stability analysis are also given here.

Finally, the contributed papers appear in the third part of the thesis.

Chapter 2

Wastewater Treatment Plants

This chapter provides a general description of municipal WWTPs. The key parts and processes are presented, so as to understand the resulting identification and control tasks. The focus is on the biological treatment part of a WWTP, which is implemented as an ASP and hence also presented along with a benchmark model used for simulations and data generation.

2.1 General Description

Nowadays, a typical WWTP is a very complex facility with various hardware system, technological processes, chemical and biological reactions. The influent wastewater may carry sewage from households and the public sector, possibly combined with storm water and wastewater from industries. However, industries are often obliged to have their own wastewater pre-treatment processes before discharging the sewage into common WWTPs.

As a result, wastewater in general contains a lot of debris of different nature: particles, organic matters and chemicals, [32] and [38]. The first task is to remove bigger waste components during a mechanical treatment using different grids and filters. Then, the biological treatment follows. Organic materials are removed from the wastewater using mainly aerobic biological processes, i.e. microorganisms (or bacteria) are engaged to deplete biodegradable soluble organic elements. The final part is to perform a chemical treatment in order to reduce the amount of phosphorous in the wastewater. In addition, the sludge that is obtained during a sedimentation process is treated separately when the water content is being reduced and digested sludge and biogas are produced.

A schematic representation of the process described above is shown

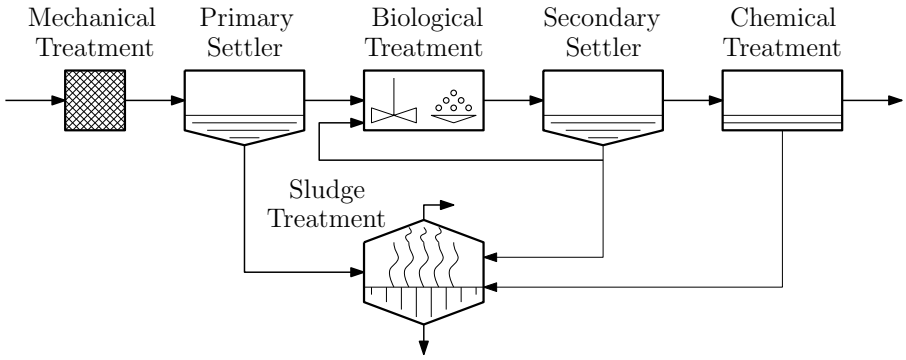

Figure 2.1: A schematic representation of a typical WWTP.

in Fig. 2.1. The focus of this work lies within the biological treatment part and the secondary settler and it is described in more detail below.

2.2 The Activated Sludge Process

The activated sludge process is a substantial part of the biological treatment commonly used in various WWT plants, [12] and [15]. It consists of a number of bioreactors, anoxic and anaerobic, as well as a secondary settler. The aerobic compartments are of particular interest in this work.

A typical aerobic bioreactor makes use of bacteria which consume organics and need a supply of DO for reproduction. One of the ways to provide oxygen in a wastewater treatment process is to use oxygen diffusers installed inside an aerobic bioreactor. The air is pumped through a valve into the wastewater creating bubbles. To provide the required DO level in the wastewater, the valve opening is controlled. A basic activated sludge

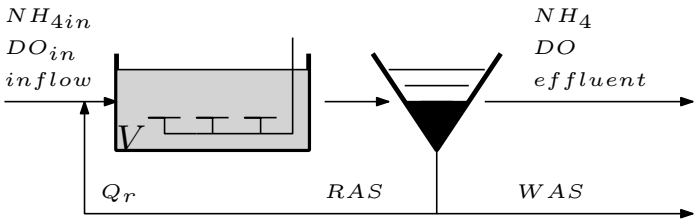

Figure 2.2: A basic activated sludge process with one aerated bioreactor and a settler. RAS - return activated sludge, WAS - waste activated sludge.

process structure is shown in Fig. 2.2.

One of the models used to describe the ASP dynamics is the Activated Sludge Model no.1 (ASM1), which was introduced in 1983 by the International Water Organisation, [13] and [14]. The ASM1 represents a mathematical model for nitrification, carbon oxidation and denitrification processes in the ASP. The model is based on 19 model parameters, 13 process variables and 8 process equations and is widely used for dynamical modelling of ASPs.

The following differential equations are often used to describe the relation between DO and ammonium variables:

$$\frac{dNH_4}{dt} = -\frac{\mu}{Y}X + \frac{Q_{in}}{V}NH_{4in} + \frac{Q_r}{V}NH_4 - \frac{Q_{in}+Q_r}{V}NH_4, \tag{2.1}$$

$$\frac{dDO}{dt} = -\frac{4.57-Y}{Y}\mu X - \frac{Q_{in}+Q_r}{V}DO + K_La(DO_{sat} - DO), \tag{2.2}$$

where X, NH_4, DO are biomass, ammonium and oxygen concentrations respectively, Q_r is the return flow, V is the volume, Q_{in} is the inflow, Y is the yield coefficient, NH_{4in} is the influent ammonium concentration, DO_{sat} is the saturation level for DO, K_La -is the oxygen transfer function describing the rate of the oxygen transfer by the aeration system.

The specific growth rate, μ, is described by the Monod equation, [6] and [26], and relates the growth rate to the DO concentration as follow

$$\mu = \mu_{max}\frac{NH_4}{(k_{NH_4} + NH_4)}\frac{DO}{(k_o + DO)}, \tag{2.3}$$

where, μ_{max} is the maximum specific growth rate, k_{NH_4} and k_o are half-saturation constants for ammonium and DO, respectively.

2.3 The Benchmark Simulation Model no.1

The complexity and variety of components and parameters in an ASP makes it a challenging task to control and simulate the process. For that reason, a simulation model, the Benchmark Simulation Model no.1 (BSM1), was created to allow evaluation and test of control strategies, parameter variations and model estimation methods, [6]. The simulation model represents a typical ASP with anoxic and anaerobic compartments and it consists of five bioreactors and a clarifier (settler). Two out of five of the bioreactors are anoxic and the remaining three bioreactors are anaerobic.

There are influent data files used in the benchmark model that are designed for various weather conditions: dry, rainy and stormy weather. These settings allow a reasonable evaluation of the system with respect to realistic environmental variables.

2.3.1 Reduced Simulation Models

In this thesis, the study is based on two simplified versions of the BSM1. In the first simplified model, the anoxic section is neglected and the aeration section consists of one bioreactor with a volume of approximately 4000 m^3. This setting is used in Papers I and II.

The second simplified simulation model also disregards the anoxic part of the ASP, but the aerated section is increased to three bioreactors with smaller volumes. Papers III and IV are based on this simulation model.

Chapter 3

System Identification, Control and Stability Analysis

This chapter gives a brief review of the system identification field along with an introduction to automatic control and the stability analysis relevant for the thesis. These tools will then be applied to the studied control problem. It does not serve as a complete description of the areas but rather aims to outline certain topics to facilitate the reading of the thesis.

3.1 System Identification

The goal of system identification is to estimate models of dynamical systems using measured data, [21], [31] and [36]. This area has been studied extensively and used in many applications, see e.g. [5], [27] and [28]. The purpose of system identification is in general to obtain a simple but accurate description of a dynamic system which provides an opportunity to study and to manipulate the system for the desired purposes, like control.

Fig. 3.1 shows a schematic description of a dynamic system. A typical scenario is to perform the modelling of the system based on input and output data sets only. However, this may not be the case in the majority of the practical applications. Hence, a disturbance (sometimes modelled as white noise) is often added to the model of the system in order to describe the influence from unknown or partly known variables, unmodelled dynamics and sensor noise. During identification, the input data may be generated either by a plant or by a user, with the output being measured at the points of interest of the process.

The system represented by Fig. 3.1 can sometimes be described as a

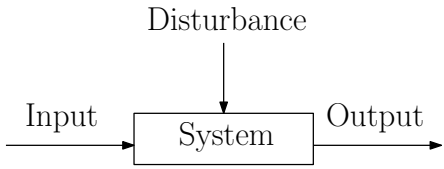

Figure 3.1: A block diagram of a dynamic system.

single-input-single-output (SISO) system, [21]. This is the most common and least complex representation and it is often used for control and analysis. Still, the majority of systems, including WWTPs, are affected by multiple external variables and are better modelled as multiple-input-single-output (MISO) or multiple-input-multiple-output (MIMO) systems when additional feedback measurements are available.

One of the aspects to consider when defining a system model is whether the model structure should be linear or nonlinear. Real world systems are seldom linear, with nonlinear effects being common in practice. However, nonlinear systems can often be well approximated by linear components (for example, by linearisation around an equilibrium point), in order to reduce the complexity and to make it possible to apply standard linear control and analysis methods. When this is not possible nonlinearities need to be embedded in the system model.

Then, a substantial part of the system identification procedure is to provide means to find the best model parameters to explain the data, [36]. Different results are obtained depending on the input signal variation, disturbance impacts and performance conditions in particular for nonlinear systems. A good model can be said to be the one that estimates the system well enough under all these limitations. The choice of the final model is often made by using a validation procedure which includes tests on another data set than was used for identification, [22]. Ideally, the model should be flexible enough to provide reliable results under all relevant operating conditions.

3.2 Model Structures and Identification Algorithms

The system identification relies on data which is usually represented as

$$Z_N = \{y(t), u(t)\}_{t=1}^{N}, \tag{3.1}$$

where $y(t)$ and $u(t)$ are output and input signals of a system, respectively, at discrete time $t = 1, ..., N$. Note that in this work, t refers to both continuous

and discrete times depending on the context.

The model structure is then used to define a predictor, p, based on the past knowledge from the data, i.e. Z_{t-1}, and the parameter vector θ, [21], and can be defined as follow

$$\hat{y}(t,\theta) = p(Z_{t-1},\theta). \tag{3.2}$$

Here, $\hat{y}(t,\theta)$ is the predicted output at time t given all data measured up to time $t-1$. The parametrization of the vector θ usually varies and depends on the model structure. Typically, its estimate is obtained by solving a minimization problem

$$\hat{\theta}_N = \underset{\theta}{\operatorname{argmin}}\, V_N(\theta), \tag{3.3}$$

where the cost function $V_N(\theta)$ differs between different identification methods. Some parametrization methods for $p(Z_{t-1},\theta)$ are presented below in this chapter.

3.2.1 Linear Models

Linear models obey the superposition principle, [19]. Therefore, the system can be described by a sum of responses to different input signals. It allows for a break down of more complex nonlinear systems using linearisation, which opens up for use of a large amount of existing system identification methods. Therefore, understanding linear systems is of fundamental importance for studying and approximating nonlinear ones.

A general linear polynomial model in the shift operator q

$$y(t) = H(q,\theta)u(t) + L(q,\theta)e(t) \tag{3.4}$$

can be applied to describe a linear system in discrete time t, where $y(t)$ is the output signal, $u(t)$ is the input signal, θ is a parameter vector, $e(t)$ is a white noise disturbance, $H(q,\theta)$ and $L(q,\theta)$ are transfer function operators describing the relationships between the output, the input and the disturbance, respectively. Here, q is the forward shift operator which operates as $qu(t) = u(t+1)$. This representation is used as arguments for transfer functions and polynomials in Papers III and IV. However, the use of a backward shift operator $q^{-1}u(t) = u(t-1)$ is also possible and was adopted in Papers I and II.

3.2.2 Output Error Identification

One common way to identify a linear system is to use the output error method for linear systems (LOE), see [21] or [36]. For the SISO case, consider

the predictor given by

$$\hat{y}(t,\theta) = H(q,\theta)u(t) = \frac{B(q,\theta)}{A(q,\theta)}u(t,\theta), \tag{3.5}$$

where

$$B(q,\theta) = b_1 q^{-n_k} + ... + b_{n_b} q^{-n_k-n_b+1}, \tag{3.6}$$

$$A(q,\theta) = 1 + a_1 q^{-1} + ... + a_{n_a} q^{-n_a}, \tag{3.7}$$

where n_k is the input delay defined by the number of samples before the input $u(t)$ affects the output $y(t)$.

Then, the parameter vector θ of (3.5) is given by the polynomial coefficients

$$\theta = \begin{bmatrix} a_1 & \cdots & a_{n_a} & b_1 & \ldots & b_{n_b} \end{bmatrix}^{\mathsf{T}} \tag{3.8}$$

and estimated so that the squared error between the measured output $y(t)$ and the predictor output $\hat{y}(t,\theta)$ of (3.5) is minimized.

For the MISO case, the output is simply defined as

$$\hat{y}(t,\theta) = \sum_{i=1}^{I} \frac{B_i(q,\theta)}{A_i(q,\theta)}u_i(t), \tag{3.9}$$

where I is the number of inputs and the polynomials $B_i(q,\theta)$ and $A_i(q,\theta)$, $i = 1, ..., I$, are given by (3.6) and (3.7), respectively.

3.2.3 Nonlinear Models

A nonlinear model is of more adequate representation of a real system when the input does not follow the output proportionally. One quite general nonlinear model has the form

$$\begin{aligned} \dot{x}(t,\theta) &= f(t, x(t,\theta), u(t), \theta), \\ \hat{y}(t,\theta) &= h(t, x(t,\theta), u(t), \theta), \end{aligned} \tag{3.10}$$

where $\dot{x}(t,\theta)$ is the state vector at time t, $u(t)$ is the input, $\hat{y}(t,\theta)$ is the output and θ is a parameter vector. Hence, the system depends nonlinearly on the past states and inputs.

The model (3.10) is significantly more complicated to handle than a linear model. The identification procedure therefore also tends to be more complex. A further reason to consider more simple model structures is the fact that systematic controller design based on an estimated model like (3.10)

also becomes much more advanced than when linear systems are treated. It is therefore of interest to study less complicated models, and to investigate if they are sufficient for solution of the ammonium control problem in ASPs.

One possibility is to treat a nonlinear system as a combination of nonlinear and linear elements, so called block-oriented models [11], [18]. Block-oriented models belong to a class of models, where the connection between input and output signals can be described by combinations of linear dynamics and static nonlinear functions. The model structure is defined by the location of each element within the system. The most well-known block-oriented models structures are

- Wiener models, which represent the system as a linear dynamic model followed by a static nonlinear function, [35].
- Hammerstein models, which represent the system with a linear dynamic element placed after a nonlinear static function, [4].
- Hammerstein-Wiener models are a combination of the above models. The linear dynamics is surrounded by two static nonlinearities.
- Wiener-Hammerstein models enclose a static nonlinearity model between two linear dynamic blocks.

The Hammerstein model structure is studied in more details in this thesis.

3.2.4 The Hammerstein Model Structure

A SISO Hammerstein model is shown in Fig. 3.2. It is given as a combination of two submodels: a nonlinear static function and a linear dynamic model. The predictor can be written as

$$\hat{y}(t,\theta) = \frac{B(q,\theta_l)}{A(q,\theta_l)} u_n(t,\theta_n), \tag{3.11}$$

where $B(q,\theta_l)$ and $A(q,\theta_l)$ are the polynomials given by

$$B(q,\theta_l) = b_1 q^{-n_k} + ... + b_{n_b} q^{-n_k-n_b+1}, \tag{3.12}$$

$$A(q,\theta_l) = 1 + a_1 q^{-1} + ... + a_{n_a} q^{-n_a}, \tag{3.13}$$

n_k is the input delay and θ_l and θ_n are parameter vectors of the linear model and nonlinear function, respectively.

The function $u_n(t,\theta_n)$ is a static nonlinearity described by

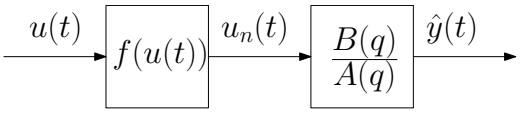

Figure 3.2: A Hammerstein model.

$$u_n(t, \theta_n) = f(u(t), \theta_n), \tag{3.14}$$

where θ_n is a vector of parameters used to describe the nonlinear function and t is discrete time. All parameters can be described by the vector

$$\theta = \begin{bmatrix} \theta_n \\ \theta_l \end{bmatrix}. \tag{3.15}$$

The parameter vector θ_l of a linear part is expressed as a vector of polynomial coefficients, (3.8).

Since the selection of the static nonlinearity is of specific importance for the thesis, these details are collected in a separate subsection below.

3.2.5 Gauss-Newton Algorithm for Parameter Estimation

There are a number of parameter estimation methods available in the system identification literature, and the prediction error method (PEM) is one of the most general and popular techniques, [21] and [36]. This offline estimation method minimizes the following criterion

$$V_N(\theta) = \frac{1}{N} \sum_{t=1}^{N} \varepsilon^2(t, \theta), \tag{3.16}$$

where

$$\varepsilon(t, \theta) = y(t) - \hat{y}(t, \theta) \tag{3.17}$$

is the prediction error.

In order to obtain a minimum of $V_N(\theta)$, the Gauss-Newton algorithm can be applied. The minimization procedure then iterates a numerical loop starting from an initial estimate $\hat{\theta}^{(0)}$ and proceeding according to

$$\hat{\theta}^{(k+1)} = \hat{\theta}^{(k)} + \alpha_k R^{-1}(\hat{\theta}^{(k)}) \sum_{t=1}^{N} \psi(t, \hat{\theta}^{(k)}) \varepsilon(t, \hat{\theta}^{(k)}), \tag{3.18}$$

where α_k is the step-length, $\psi(t, \hat{\theta}^{(k)})$ is the negative gradient of $V(\theta)$ with respect to θ and the Hessian $R(\hat{\theta}^{(k)})$ is given by

$$R(\hat{\theta}^{(k)}) = \frac{1}{N}\sum_{t=1}^{N}\psi(t,\theta)\psi^{\mathsf{T}}(t,\theta). \tag{3.19}$$

3.2.6 Hammerstein Model Based RPEM

Another way to estimate the parameters is to apply recursive algorithms which can be performed online using states and parameter estimates from a previous time step $(t-1)$, [21] and [36]. This gives an inherent advantage when it comes to tracking dynamic process changes. A recursive prediction error method (RPEM) for minimizing (3.16) was developed by [24] and is also used in this thesis.

Assume that the static nonlinearity is piecewise linear with a grid $\mathcal{G}$ defining the breakpoints between linear intervals. If the grid $\mathcal{G}$ has predefined and fixed points, then the gradient in (3.18) can be described as

$$\psi(t,\theta) = \left[\frac{d}{d\theta}\hat{y}(t,\theta)\right]^{\mathsf{T}} = \begin{bmatrix} \frac{B(q^{-1})}{A(q^{-1})}F(u(t),\mathcal{G}) \\ \frac{1}{A(q^{-1})}\varphi(t,\theta) \end{bmatrix}, \tag{3.20}$$

where $F(u(t),\mathcal{G})$ is further defined in (3.22) .

Shortly, the algorithm then follows as

$$\begin{aligned}
\varepsilon(t) &= y(t) - \hat{y}(t) \\
R(t) &= R(t-1) + \frac{1}{t}\Big(\psi(t)\psi^{\mathsf{T}}(t) - R(t-1)\Big) \\
\hat{\theta}(t) &= \hat{\theta}(t-1) + \frac{1}{t}R^{-1}(t)\psi(t)\varepsilon(t) \\
\varphi(t+1) &= [-\hat{y}(t) \quad \cdots \quad -\hat{y}(t-n_a+1) \\
&\qquad f(u(t-n_k+1),\hat{\theta}(t)) \quad \cdots \\
&\qquad f(u(t-n_k-n_b+2),\hat{\theta}(t))]^{\mathsf{T}} \\
\psi(t+1) &= \begin{bmatrix} \frac{\hat{B}(q^{-1},t)}{\hat{A}(q^{-1},t)}F(u(t+1),\mathcal{G}) \\ \frac{1}{\hat{A}(q^{-1},t)}\varphi(t+1) \end{bmatrix} \\
\hat{y}(t+1) &= \hat{\theta}_l^{\mathsf{T}}\varphi(t+1).
\end{aligned} \tag{3.21}$$

For more details and proofs of convergence see [23] and [25].

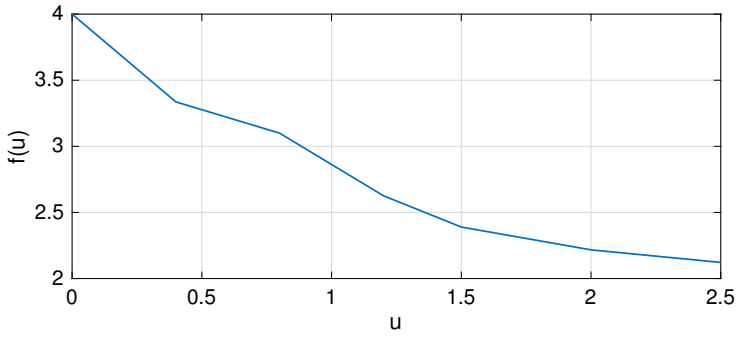

Figure 3.3: An example of a piecewise linear function.

3.2.7 Static Nonlinearities

The nonlinear parameter vector θ_n in (3.15) is defined by the type of the nonlinearity incorporated in the Hammerstein model. In this thesis, two types of nonlinearities are studied.

The first one is a piecewise linear function. A nonlinear function can be approximated as a set of connected linear functions, i.e. a piecewise linear function. A sample function is shown in Fig.3.3. Every piecewise linear function between consecutive points can be expressed as

$$f(u, \theta_n) = \sum_{i=1}^{n_r} r_i f_i(u, \mathcal{G}) = \theta_n^{\mathsf{T}} F(u, \mathcal{G}), \tag{3.22}$$

where $f_i(u, \mathcal{G})$ are piecewise affine basis functions, and

$$\begin{aligned} \theta_n &= \begin{bmatrix} r_1 & \dots & r_{n_r} \end{bmatrix}^{\mathsf{T}}, \\ F(u, \mathcal{G}) &= \begin{bmatrix} f_1(u, \mathcal{G}) & \cdots & f_{n_r}(u, \mathcal{G}) \end{bmatrix}. \end{aligned} \tag{3.23}$$

The grid $\mathcal{G} = \begin{bmatrix} u_1 & \cdots & u_{n_r} \end{bmatrix}$ assigns positions of connecting points between every two linear functions, and every parameter in θ_n describes the value of a function.

The second type of nonlinearity considered is inspired by the Monod function, (2.3), [26], which can be integrated in the model as a part of the nonlinear subsystem in Fig. 3.2. This choice is less general and is tailored for the application of the thesis.

A Monod function is shown in Fig. 3.4 and it can be written in a general form as

$$\mu = \mu_{max} \frac{\chi}{\chi + k_\chi}, \tag{3.24}$$

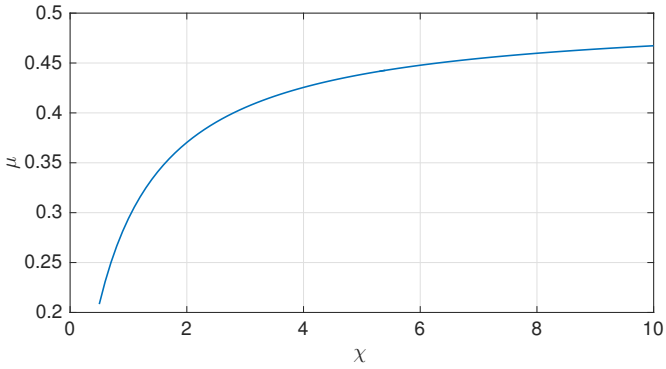

Figure 3.4: An example of a Monod function.

where μ is used to describe the growth of the biomass, μ_{max} is a maximum growth rate usually fixed to a constant value, χ is a current concentration of the substrate and k_χ is a fixed saturation constant associated with this substrate.

Also, some other type of simple nonlinear functions can be applied and they are presented in Paper II.

3.3 Ammonium-based Aeration Control in WWTPs

As discussed in Chapter 1, ammonium-based aeration control is becoming a popular technique to apply in ASPs to save energy and improve nitrogen removal, [16] and [34]. Therefore, NH_4 concentration measurements from installed sensors are used for DO concentration control in all aeration zones.

When the ammonium concentration level is too high, the control strategy is to increase the aeration and hence to increase the DO level, which leads to a NH_4 decrease. However, such control is sufficient only for a certain range of DO concentration due to a nonlinearity of the nitrification process: when the DO value increases, the efficiency is reduced.

Typically, inner feedback controllers are implemented in aerated bioreactors to maintain the DO at a certain level. In addition, measuring the influent loads and disturbances may contribute to the control efficiency. Therefore, combining feedback and feedforward control could result in an improved ammonium control.

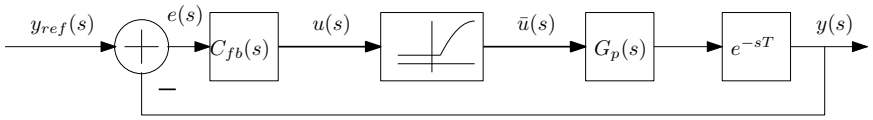

Figure 3.5: A block diagram representation of a feedback control system suitable for ammonium control. The notation is explained in the text.

3.3.1 Feedback Controller Design

In Fig. 3.5, the schematic representation of a simple closed loop feedback system, relevant for ammonium control, is shown. Since the design and stability analysis use continuous time tools, the following presentation is given in terms of continuous time, using the Laplace transform variable s, when discussing frequency properties. The input to the nonlinear system is governed by a controller $C_{fb}(s)$ which operates on the control error $e(s)$ to give an input $u(s)$. The control loop is effected by a process time delay T. The system also incorporates a saturation. This structure is used in the present thesis, together with feedforward control. The static nonlinearity is given by

$$\bar{u}(t) = \begin{cases} f(u_{max}), & u(t) \geq u_{max} \\ f(u(t)), & u_{min} < u(t) < u_{max} \\ f(u_{min}), & u(t) \leq u_{min}. \end{cases} \tag{3.25}$$

As shown in [43] and [44], the saturation may lead to stability problems if the low frequency gain is selected too high. The approach is then to use a leaky proportional-integral (PI) controller. PI controllers are typically applied in the WWTP area due to their simplicity and a wide area of application. In order to limit the low frequency loop gain, leakage is added to the integrator part of a PI-controller, [43], as follow

$$C_{fb}(s) = K_P + K_I \frac{1}{s + \alpha}, \tag{3.26}$$

where α is a leakage with K_P and K_I being proportional and integral gains, respectively. This controller enables the use of input-output stability theory for analysing the closed loop stability properties.

3.3.2 Feedforward Controller Design

A feedforward controller is typically used to eliminate or to significantly reduce the effect of a disturbance on a system. Therefore, the ideal feedfor-

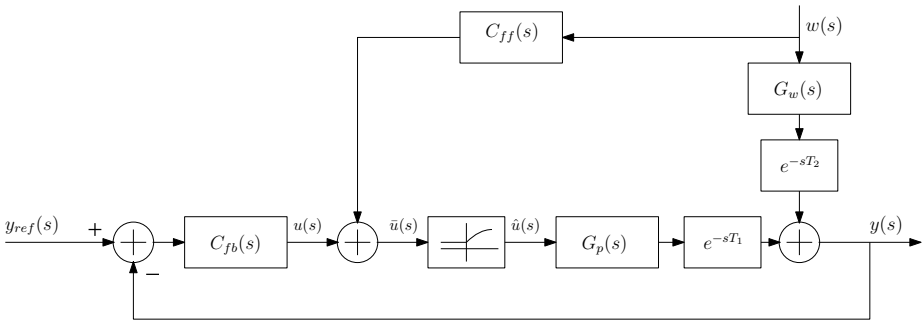

Figure 3.6: A block diagram representation of a combined feedback and feedforward control system suitable for ammonium control.

ward controller is based on a perfect disturbance rejection, when a controller is designed to make the overall effects of disturbances negligible. To achieve this, the controller can be selected as

$$K_m \frac{G_w(s)}{G_p(s)} e^{-s(T_2-T_1)} \approx -K_m \frac{G_w(s)}{G_p(s)} = C_{ff}(s), \tag{3.27}$$

$G_w(s)$ is the disturbance transfer function and $G_p(s)$ is the plant transfer function of the block diagram of Fig. 3.6, K_m is the gain of the nonlinearity at a selected operating point. The time delay is neglected in (3.27) since if $T_1 > T_2$ the controller would become infeasible. Another possibility would be to introduce prediction.

In the ASP, aeration control may be affected by variations in an influent load, [33], and omitting the disturbance can impact the performance of a single feedback controller considerably. Hence, the feedforward controller is commonly implemented along with the feedback one in order to improve the overall efficiency of the control system.

The feedback and feedforward controllers are designed individually and the feedforward loop does not effect the stability of the closed loop system.

3.4 Stability Analysis of the Simplified ASP Model

A number of effects in the ASP, like the highly nonlinear behaviour, can lead to an uncertain model. Additionally, the presence of saturation and time delays may complicate the controller design. Therefore, a significant low frequency gain of the loop is beneficial to ensure an accurate regulation.

However, as discussed above and proved in [43] and [44], this may have a negative effect on stability. There are different methods to investigate the stability properties of the system, here the Popov criterion is used and

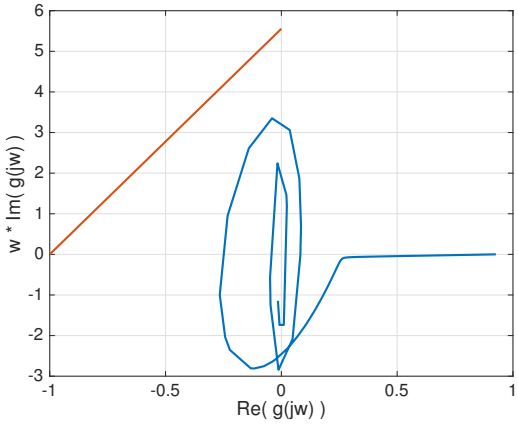

Figure 3.7: An example of the Popov criterion with $k = 1$.

$\mathcal{L}_2$-stability regions are pre-computed to ensure a stable feedback controller. The $\mathcal{L}_2$-stability is defined in more detail in Paper III.

3.4.1 Popov Criterion

The linear part of the loop gain of the system in Fig. 3.5 is given by

$$\hat{g}(s) = e^{-sT_1} C_{fb}(s) G_p(s), \tag{3.28}$$

Under conditions given in the papers of the thesis, the Popov criterion can be applied to define the stability region of the system.

Following [40], the Popov criterion is defined by the Popov plot

$$\omega \in [0, \infty) \rightarrow Re[\hat{g}(j\omega)] + j\omega Im[\hat{g}(j\omega)] \in C, \tag{3.29}$$

which should lie entirely to the right of a line through $-1/k + \delta + j0$ with a slope $1/q$, for some $q \geq 0$ and some $\delta > 0$. If this is the case, the system is $\mathcal{L}_2$-stable, an the stability region is determined by the Popov inequality

$$Re[(1 + j\omega q)\hat{g}(j\omega)] + \frac{1}{k} \geq \delta > 0, \ \forall \omega \geq 0 \text{ and } q > 0. \tag{3.30}$$

Fig. 3.7 illustrates an example of a Popov plot when the Popov inequality is fulfilled.

3.4.2 Precomputation of the Stability Region

The stability region for $\hat{g}(s)$, (3.28), can be calculated as a function of a set of controller parameters represented by the proportional gain K_P, the

integral gain K_I and the leakage α. The precomputations of the stability region were first described in [44] and [45].

The procedure is outlined in Algorithm 1. The stability region pre-computations are defined by parameters and uncertainty grids for the maximum allowed time delay T_{max}. The calculations building on the Popov inequality (3.30) are performed over all parameters combinations until the inequality does not hold. When no line can be drawn on the left side of the Popov plot, the stability region border is reached and the maximum allowed time delay is determined.

A more detailed description of computations and results are presented in Papers III and IV.

Algorithm 1 Stability region pre-computation

Parameter grid $[P_1...P_i]$, delay grid $[T_1...T_j]$, line grid $[q_1...q_m]$, frequency grid $[\omega_1...\omega_n]$
for $P = P_1, ..., P_i$ **do**
  for $T = T_1, ..., T_j$ **do**
    $found_q = 0$
    for $q = q_1, ..., q_m$ **do**
      for $\omega = \omega_1, ..., \omega_n$ **do**
        $\hat{g}(jw) = e^{-jwT} C_{fb}(jw) G_p(jw)$
      end for
      if $Re[\hat{g}(j\omega)] + qj\omega Im[\hat{g}(j\omega)] > -1/k \ \forall \ \omega$ **then**
        $found_q = 1$
      end if
    end for
    if $found_q = 0$ **then**
      $T_{max}(P) = T$
      $break$
    end if
  end for
end for

Chapter 4

Concluding Remarks

4.1 Discussion

The study conducted in this thesis consists of two major parts. The first part concerns identification of the activated sludge process aiming to describe the relationship between the dissolved oxygen and ammonium concentration. The nonlinear grey-box model was shown to give the best system identification and it was therefore used in the next step of the study.

Based on the identified model, controller design was conducted. The nonlinear dynamics, process saturations and time delays affect the system, making it challenging to provide a stable loop. Therefore, the feedback controller was designed and tuned ensuring a stable closed loop system.

Finally, the influence of disturbances on the system was studied leading to an introduction of a feedforward controller. The combination of feedback and feedforward controllers provided an improved closed loop performance and contributed to a significantly improved disturbance rejection.

4.2 Future work

The experiments were performed on a simplified version of an activated sludge process model. The natural next step is to test the proposed methods on a complete original Benchmark Simulation Model no.1. Then, the data obtained from a real plant should be studied and used for system identification. Finally, the proposed methods should be tested on a pilot plant under various conditions.

Bibliography

[1] L. Åmand, *Ammonium feedback control in wastewater treatment plants*, Ph.D. thesis, Uppsala University, Uppsala, Sweden, 2014.

[2] L. Åmand, G. Olsson, and B. Carlsson, *Aeration control - a review*, Water Science and Technology **67** (2013), no. 11, 2374–2398.

[3] K.J. Åström and T. Hägglund, *Advanced PID Control*, ISA -The Instrumentation, Systems, and Automation Society, 2006.

[4] E.-W. Bai and M. Fu, *A blind approach to Hammerstein model identification*, IEEE Transactions on Signal Processing **50** (2002), no. 7, 1610–1619.

[5] L. Brus, *Nonlinear identification of a solar heating system*, Proceedings of 2005 IEEE Conference on Control Applications, CCA 2005, 2005, pp. 1491–1497.

[6] J. B. Copp, *The COST simulation benchmark: Description and simulator manual*, Office for Official Publications of the European Community, Luxemburg, 2002.

[7] A. C. B. de Araújo, S. Gallani, M. Mulas, and G. Olsson, *Systematic approach to the design of operation and control policies in activated sludge systems*, Industrial & Engineering Chemistry Research **14** (2011), no. 50, 8542–8557.

[8] M. Ekman, *Bilinear black-box identification and MPC of the activated sludge process*, Journal of Process Control **18** (2008), no. 7, 643–653.

[9] Water Environment Federation, *Energy conservation in water and wastewater facilities*, McGraw-Hill, 2010.

[10] M. H. Gerardi, *Nitrification and denitrification in the activated sludge process*, John Wiley & Sons, 2003.

[11] F. Giri and E.-W. Bai, *Block-oriented nonlinear system identification*, vol. 1, Springer, London, 2010.

[12] M. J. Hammer and M. J. Hammer Jr., *Water and wastewater technology*, Prentice Hall, 2012.

[13] M. Henze, *Activated sludge model no. 1*, IAWPRC Scientific and Technical Reports **1** (1987).

[14] M. Henze, W. Gujer, T. Mino, and M. van Loosdrecht, *Activated sludge models*, Scientific and Technical Report Series, IWA Publishing, 2000.

[15] M. Henze, M. C. M. van Loosdrecht, G. A. Ekama, and D. Brdjanovic, *Biological wastewater treatment*, IWA Publishing, 2008.

[16] P. Ingildsen, U. Jeppsson, and G. Olsson, *Dissolved oxygen controller based on on-line measurements of ammonium combining feed-forward and feedback*, Water Science & Technology **45** (2002), no. 4-5, 453–460.

[17] U. Jeppsson, J. Alex, M. N. Pons, H. Spanjers, and P. Vanrolleghem, *Status and future trends of ICA in wastewater treatment - a European perspective*, Water Science & Technology **45** (2002), no. 4-5, 485–494.

[18] R. K. Pearson and M. Pottmann, *Grey-box identification of block-oriented nonlinear models*, Journal of Process Control **10** (2000), 301–315.

[19] T. Kailath, *Linear systems*, Information and System Sciences Series, Prentice-Hall, 1980.

[20] C.-F. Lindberg, *Multivariable modeling and control of an activated sludge process*, Water Science & Technology **37** (1998), no. 12, 149–156.

[21] L. Ljung, *System identification: Theory for the user (2nd ed.)*, Prentice Hall, Upper Saddle River, NJ, USA, 1999.

[22] _____, *System identification toolbox: Users guide version 7.4*, Natick, MA, USA: The Mathworks, 2011.

[23] P. Mattsson, *Modelling and identification of nonlinear and impulsive systems*, Ph.D. thesis, Uppsala University, Uppsala, Sweden, 2016.

[24] P. Mattsson and T. Wigren, *Recursive identification of Hammerstein models*, American Control Conference, 2014, pp. 2498–2503.

[25] ———, *Convergence analysis for recursive Hammerstein identification*, Automatica **71** (2016), 179–186.

[26] J. Monod, *The growth of bacterial cultures*, Annual Review of Microbiology **3** (1949), 371–394.

[27] E. A. Morelli and V. Klein, *Application of system identification to aircraft at NASA langley research center*, Journal of Aircraft **42** (2005), no. 1, 12–25.

[28] M. Mulas, S. Tronci, F. Corona, H. Haimi, P. Lindell, M. Heinonen, R. Vahala, and R. Baratti, *An application of predictive control to the Viikinmäki wastewater treatment plant*, Journal of Process Control **35** (2015), 89 – 100.

[29] M. O'Brien, J. Mack, B. Lennox, D. Lovett, and A. Wall, *Model predictive control of an activated sludge process: A case study*, Control Engineering Practice **19** (2011), no. 1, 54–61.

[30] G. Olsson, M. Nielsen, Z. Yuan, A. Lynggaard-Jensen, and J. P. Steyer, *Instrumentation, control and automation in wastewater systems*, Scientific and Technical Report Series, IWA Publishing, 2005.

[31] R. Pintelon and J. Schoukens, *System identification: A frequency domain approach*, Wiley, New Jersey, USA, 2012.

[32] D. G. Rao, R. Senthilkumar, J. A. Byrne, and S. Feroz, *Wastewater treatment: Advanced processes and technologies*, CRC Press, 2012.

[33] L. Rieger, R. M. Jones, P. L. Dold, and C. B. Bott, *Myths about ammonia feedforward aeration control*, Proceedings of the Water Environment Federation **9** (2012).

[34] ———, *Ammonia-based feedforward and feedback aeration control in activated sludge processes*, Water Environment Research **86** (2014), 63–73.

[35] M. Schetzen, *The Volterra and Wiener theories of nonlinear systems*, Wiley, 1980.

[36] T. Söderström and P. Stoica, *System identification*, Prentice-Hall, Inc., Hemel Hempstead, UK, 1989.

[37] O. A. Z. Sotomayor, S. W. Park, and C. Garcia, *Multivariable identification of an activated sludge process with subspace based algorithms*, Control Engineering Practice **11** (2003), 961–969.

[38] R. M. Stuetz and T. Stephenson, *Principles of water and wastewater treatment processes*, Water and Wastewater Process Technologies Series, IWA Publishing, 2009.

[39] D. F. Tilley, *Aerobic wastewater treatment processes*, IWA Publishing, 2011.

[40] M. Vidyasagar, *Nonlinear Systems Analysis*, Prentice Hall, London, UK, 1978.

[41] D. Vrečko and N. Hvala, *Model-based control of the ammonia nitrogen removal process in a wastewater treatment plant*, Case Studies in Control: Putting Theory to Work (S. Strmčnik and Đ. Juričić, eds.), Springer London, 2013.

[42] D. Vrečko, N. Hvala, A. Stare, and S. Podbevsek, *Improvement of ammonia removal in activated sludge process with feedforward-feedback aeration controllers*, Water Sci. Technol., **4-5** (2006), no. 53, 125–132.

[43] T. Wigren, *Low-frequency limitations in saturated and delayed networked control*, Proceedings IEEE CCA 2015, Manly, Sydney, NSW, Australia, September 21–23, 2015, pp. 564–571.

[44] ———, *Low frequency sensitivity function constraints for nonlinear L2-stable networked control*, Asian J. Contr. **18** (2016), no. 4, 1200–1218.

[45] ———, *Wireless feedback and feedforward data flow control subject to rate saturation and uncertain delay*, IET Control Theory & Applications **10** (2016), no. 3, 346–353.

Paper I

Nonlinear system identification of the dissolved oxygen to effluent ammonia dynamics in an activated sludge process

Tatiana Chistiakova[1], Per Mattsson [2], Bengt Carlsson[1] and Torbjörn Wigren[1]

Abstract

Aeration of biological reactors in wastewater treatment plants is important to obtain a high removal of soluble organic matter as well as for nitrification but requires a significant use of energy. It is hence of importance to control the aeration rate, for example, by ammonium feedback control. The goal of this paper is to model the dynamics from the set point of an existing dissolved oxygen controller to effluent ammonia using two types of system identification methods for a Hammerstein model, including a newly developed recursive variant. The models are estimated and evaluated using noise corrupted data from a complex mechanistic model (Activated Sludge Model no.1). The performance of the estimated nonlinear models are compared with an estimated linear model and it is shown that the nonlinear models give a significantly better fit to the data. The resulting models may be used for adaptive control (using the recursive Hammerstein variant), gain-scheduling control, $\mathcal{L}_2$ stability analysis, and model based fault detection.

[1]Department of Information Technology, Uppsala University, SE 75105 Uppsala, Sweden

[2]Department of Electronics, Mathematics and Natural Sciences, University of Gävle, SE 80176 Gävle, Sweden

1. Introduction

Nonlinear system identification has been studied in many application areas, including neuron models and networks [25], heating systems, [5], wastewater treatment plants, [8], power system control, [3], selective catalytic reduction systems, [19], and numerous other applications. Along with the state of the art methods implemented in the MATLAB® System Identification Toolbox, a variety of approaches have been developed and implemented as black-box and grey-box identification methods, see e.g. [15], [17] and [23].

Modelling of block oriented systems is an important class within the system identification area. Such systems are used when the input-output relationship can be described by a combination of transfer functions with nonlinear static functions, [10] and [13]. The location of the nonlinear block then defines a model structure: if a linear block follows a static nonlinearity, such models are defined as Hammerstein models, and as Wiener models if vice versa. Also, the combination of both is used, i.e. Hammerstein-Wiener models.

The process of wastewater treatment (WWT) includes a large number of time-varying elements, like different flow rates and flow compositions, time delays, disturbances, and nonlinearities, [21]. Such a process complexity may cause problems while controlling and monitoring a plant. One approach is then to create a reduced mathematical model of the process which allows a simplified understanding of nonlinearities and their relation to different control strategies.

The focus of this paper is to compare an off-line method and a newly developed recursive method for identification of a Hammerstein model with an affine static input nonlinearity for modelling the nitrification dynamics in an Activated Sludge Process (ASP). To the best of the authors knowledge, Hammerstein modelling has not been applied to this type of process before.

The contribution shows that the Hammerstein model is a suitable model for this task, and that it is likely to be applicable for future controller design and stability analysis of the system. The emphasis is on methods for identification of Hammerstein models. These models can then be used to design a nonlinear controller which can be analysed using the Popov criterion for input-output stability and robustness, [6]. The differences in terms of the practical implementation of the two different Hammerstein based identification methods is pointed out.

The paper is organised as follows. Section 2 gives a description of a high fidelity wastewater treatment simulator and presents the motivation for the use of system identification. Methods used for identification are described in Section 3. The identification results are given in Section 4, followed by conclusions in Section 5.

2. Ammonium-based feedback control and modelling of the Activated Sludge Process

2.1 Overview

WWT involves a number of complex, nonlinear processes, which control and evaluation is a challenging and demanding task. A typical WWT plant consists of several steps including mechanical, biological and chemical treatment. In this study, the biological treatment is of particular interest.

During the biological treatment, nitrogen and organic materials are removed from the water using microorganisms. A typical process for biological treatment is the ASP, where oxygen supply via aeration is essential for the microorganisms to convert ammonia to nitrate (nitrification), [9]. The concentration of Dissolved Oxygen (DO) should be high enough to give a certain removal rate, but a too high DO level requires a high energy consumption and gives little increase in the removal rate due to the inherent nonlinearity of the nitrification process. A classical control strategy is therefore to keep the DO level close to a given and fixed set-point, [20]. It has also been found that the use of ammonia feedback to control the DO set-point can increase the energy efficiency without producing a higher effluent ammonium load, see [2] for some recent results.

2.2 Simulation model

The simulation model used in this study is depicted in Fig. 1. It is a simplified version of the Benchmark Simulation Model no.1 (BSM1), which is a simulation model for evaluating and testing various control strategies, parameter variations and models. BSM1 follows the characteristics of a real plant and is widely used for analysis, [7].The original BSM1 simulates five biological reactors and a clarifier, for this case study the number of reactors is reduced to one.

The dynamics of the benchmark model is based on the Activated Sludge Model no.1 (ASM1). ASM1 was created by the International Water Association (IWA) task group in 1983. The idea was to design and promote a simple but still accurate mathematical model for nitrification, carbon oxidation and denitrification in an ASP. The ASM1 contains 13 process variables, 19 model parameters and 8 process equations, [11]. Still today, the ASM1 remains the most commonly used model for dynamical modelling of ASPs.

2.3 Hammerstein model

The dissolved oxygen dynamics in the ASP is nonlinear. To achieve a good controller performance for all working conditions, a simplification of the

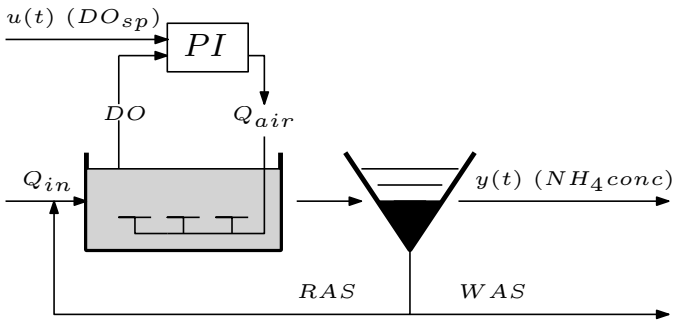

Figure 1: Simulation model. Q_{in}-inflow, $u(t)$-input signal (DO_{sp}-DO set point), PI-proportional integral DO controller, Q_{air}-airflow rate, $y(t)$-output signal (NH_4conc-ammonium concentration level) RAS-return activated sludge, WAS-waste activated sludge.

dynamic model is attempted in this paper. This is the motivation for the application of the system identification procedure in the paper.

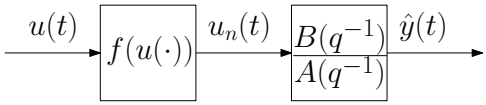

Figure 2: Hammerstein model.

A nonlinear Hammerstein model is represented by a combination of a nonlinear static and a linear dynamic submodel, see Fig. 2. In the case study, the oxygen supply can be described by a static nonlinear element followed by a linear part representing the remaining part of the plant.

The nonlinear block is defined as a static nonlinear function

$$u_n(t, \theta_n) = f(u(t), \theta_n), \tag{1}$$

where θ_n is a vector of parameters and t is discrete time. Then the output $\hat{y}(t, \theta)$ of the model can be described as

$$\hat{y}(t, \theta) = \frac{B(q^{-1})}{A(q^{-1})} u_n(t, \theta_n), \tag{2}$$

where $B(q^{-1})$ and $A(q^{-1})$ are polynomials given by

$$B(q^{-1}) = b_0 q^{-n_k} + ... + b_{n_b-1} q^{-n_k-n_b+1}, \tag{3}$$

$$A(q^{-1}) = 1 + a_1 q^{-1} + ... + a_{n_a} q^{-n_a}, \tag{4}$$

and n_k is an input delay specified by the number of samples before the output reacts to the input.

The parameters of the linear block are collected in

$$\theta_l = \begin{bmatrix} a_1 & \cdots & a_{n_a} & b_1 & \ldots & b_{n_b} \end{bmatrix}^{\mathsf{T}}. \tag{5}$$

The vector θ contains the unknown parameters, i.e.

$$\theta = \begin{bmatrix} \theta_n \\ \theta_l \end{bmatrix}. \tag{6}$$

Note that (2) can be expressed as

$$\hat{y}(t) = \theta_l^{\mathsf{T}} \varphi(t, \theta), \tag{7}$$

where

$$\begin{aligned} \varphi(t,\theta) = [&-\hat{y}(t-1,\theta) \quad \cdots \quad -\hat{y}(t-n_a,\theta) \\ &u_n(t-n_k,\theta_n) \quad \cdots \quad u_n(t-n_k-n_b+1,\theta_n)]^{\mathsf{T}}. \end{aligned} \tag{8}$$

In this contribution, the static function in (1) is modeled as a piecewise affine function. These functions are known for their universal approximation properties, see e.g. [4] and [12], and are therefore popular in system identification. Let $\mathcal{G} = \begin{bmatrix} u_1 & \cdots & u_{n_r} \end{bmatrix}$ be a set of grid points. Then any function that is piecewise affine between consecutive grid points can be written as

$$f(u, \theta_n) = \sum_{i=1}^{n_r} r_i f_i(u, \mathcal{G}) = \theta_n^{\mathsf{T}} F(u, \mathcal{G}), \tag{9}$$

where $f_i(u, \mathcal{G})$ are piecewise affine basis functions, and

$$\theta_n = \begin{bmatrix} r_1 & \ldots & r_{n_r} \end{bmatrix}^{\mathsf{T}}, \tag{10}$$

$$F(u, \mathcal{G}) = \begin{bmatrix} f_1(u, \mathcal{G}) & \cdots & f_{n_r}(u, \mathcal{G}) \end{bmatrix}. \tag{11}$$

Hence, if the grid points $\mathcal{G}$ are fixed, then the nonlinear function is linear in the unknown parameters. For an example of how the basis functions can be constructed, see e.g. [16]. It is stressed that both evaluated Hammerstein methods utilize piecewise affine parametrizations. The reason is that extended tests revealed that the piecewise affine parametrization gave the best performance.

2.4 Possible application of the Hammerstein model for control

Using a Hammerstein model, a main idea of the nonlinear feedback controller design is to introduce global stability by making use of input-output stability theory, [22]. A lag controller can then be applied so that the Popov criterion is met, cf. [26]. Alternatively, a leakage can be added to the integrator of a PI-controller. The controller may therefore be designed as

$$C(s) = K_P + K_I \frac{1}{s+\alpha}. \tag{12}$$

The block diagram of this control system is shown in Fig. 3. The controller $C(s)$ operates on the control error $e(s)$ to give a reference value for the DO level, denoted $u(s)$ in continuous time. The saturated output signal $\bar{u}(s)$ corresponds to $u_n(t)$ in discrete time in (1).

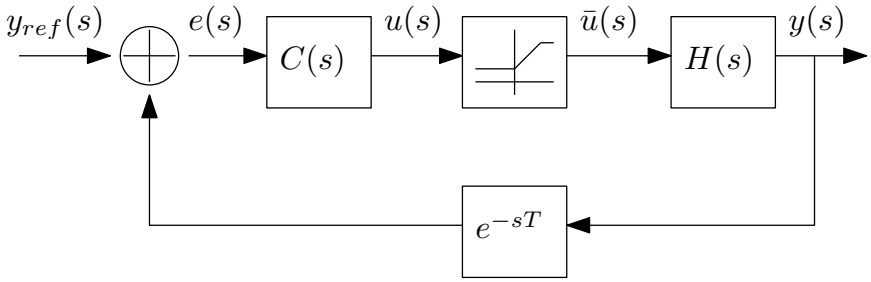

Figure 3: Block diagram of the control system.

The control signal represented by the DO set point is constrained to be between given minimum and maximum values. The imposed limitations together with the plant model nonlinearity hence give the following saturation type static nonlinearity

$$\bar{u} = \zeta(u) = \begin{cases} f(u_{max}), & u \geq u_{max} \\ f(u), & u_{min} < u < u_{max} \\ f(u_{min}), & u \leq u_{min}. \end{cases} \tag{13}$$

The saturated control signal $\bar{u}(s)$ describes the DO-concentration set point. The linear part of a plant dynamics, $H(s)$, models the dynamic effect of the DO on the ammonium concentration effluent water, denoted $y(s)$. To close the feedback loop, $y(s)$ needs to be measured. This process involves the measurement delay T.

As a continuous time delay is infinite dimensional, input-output stability theory is suitable to analyse the control system. Since the linear part of the loop gain is given by

$$\hat{g}(s) = e^{-sT} C(s) H(s), \tag{14}$$

it follows that $\hat{g}(s)$ has all poles strictly in the interior of the left half of the complex plane provided that $H(s)$ is asymptotically stable. The conclusion is that the Popov criterion is applicable, see Theorem 6.7.63 in [26]. The details of this controller design and the associated stability results are, however, not within the scope of this paper and they are reported in [6].

3. Identification methods

The scope of the paper is to apply and compare one linear and two Hammerstein based identification methods for the ASP. These methods are presented next.

3.1 The linear output error method

For identifying the linear output error (OE) model, i.e. (2) with $u_n(t,\theta) = u(t)$, the MATLAB® function *oe* was used for the Gauss-Newton optimization. See [14] for a detailed explanation of this function.

3.2 The off-line prediction error method for the Hammerstein model

The off-line prediction error method (PEM), see e.g. [13] and [18], can be applied to quite arbitrary model parameterizations, and is one of the most popular methods in system identification. In PEM, with a quadratic criterion, the goal is to minimize the cost function

$$V(\theta) = \frac{1}{N}\sum_{t=1}^{N}\varepsilon^2(t,\theta), \tag{15}$$

where

$$\varepsilon(t,\theta) = y(t) - \hat{y}(t,\theta) \tag{16}$$

is the prediction error.

In the numerical results in Section 4.2 the Gauss-Newton method is applied in order to minimize the non-convex function $V(\theta)$. That is, the algorithm is started with an initial estimate $\hat{\theta}^{(0)}$, and iterated according to

$$\hat{\theta}^{(k+1)} = \hat{\theta}^{(k)} + \alpha_k R^{-1}(\hat{\theta}^{(k)})\sum_{t=1}^{N}\psi(t,\hat{\theta}^{(k)})\varepsilon(t,\hat{\theta}^{(k)}), \tag{17}$$

where α_k is the step-length, $\psi(t,\hat{\theta}^{(k)})$ is the negative gradient of $V(\theta)$ and $R(\theta)$ is given by

$$R(\theta) = \frac{1}{N}\sum_{t=1}^{N}\psi(t,\theta)\psi^{\mathsf{T}}(t,\theta). \tag{18}$$

In the numerical examples, the MATLAB® function *nlhw*, see [14] for more details, with piecewise affine nonlinearity was used for performing the Gauss-Newton optimization for the off-line PEM. This function also optimizes the location of the grid points, so the negative gradient is then extended with derivatives with respect to the grid points as in [1]. This is a main difference as compared to the method of Section 3.3.

3.3 The recursive prediction error method for the Hammerstein model

In [15], a recursive prediction error method (RPEM) for Hammerstein identification was developed by using running estimates of the quantities of (17). A recursive identification method opens up the possibilities for using adaptive control strategies, and also for performing low complexity online fault detection. In [15], it was shown that the negative gradient for the Hammerstein model with fixed grid points in the nonlinearity, can be computed as

$$\psi(t,\theta) = \left[\frac{d}{d\theta}\hat{y}(t,\theta)\right]^{\mathsf{T}} = \begin{bmatrix} \frac{B(q^{-1})}{A(q^{-1})}F(u(t),\mathcal{G}) \\ \frac{1}{A(q^{-1})}\varphi(t,\theta) \end{bmatrix}. \tag{19}$$

The resulting algorithm can be summarized as follows

$$\begin{aligned} \varepsilon(t) &= y(t) - \hat{y}(t) \\ R(t) &= R(t-1) + \frac{1}{t}\Big(\psi(t)\psi^{\mathsf{T}}(t) - R(t-1)\Big) \\ \hat{\theta}(t) &= \hat{\theta}(t-1) + \frac{1}{t}R^{-1}(t)\psi(t)\varepsilon(t) \\ \varphi(t+1) &= [-\hat{y}(t) \quad \cdots \quad -\hat{y}(t-n_a+1) \\ &\qquad f(u(t-n_k+1),\hat{\theta}(t)) \quad \cdots \\ &\qquad f(u(t-n_k-n_b+2),\hat{\theta}(t))]^{\mathsf{T}} \\ \psi(t+1) &= \begin{bmatrix} \frac{\hat{B}(q^{-1},t)}{\hat{A}(q^{-1},t)}F(u(t+1),\mathcal{G}) \\ \frac{1}{\hat{A}(q^{-1},t)}\varphi(t+1) \end{bmatrix} \\ \hat{y}(t+1) &= \hat{\theta}_l^{\mathsf{T}}\varphi(t+1). \end{aligned} \tag{20}$$

In order to avoid the computation of $R^{-1}(t)$ in each time-step of the algorithm, it is possible to apply the matrix inversion lemma and compute $P(t) = \frac{1}{t}R^{-1}(t)$ recursively instead, see [15] for details about the implementation of the algorithm. The algorithm (20) makes use of fixed preselected grid points.

4. Numerical examples

4.1 Simulated data

The high fidelity simulator described in Section 2.2 was used for data generation. The DO set point, $u(t)$, was generated as a pseudorandom binary sequence (PRBS) multiplied by a uniformly distributed random process, with an added white noise. The so obtained sequence is hence a sequence where each constant interval is multiplied with a uniformly distributed amplitude, see [24] for more details.

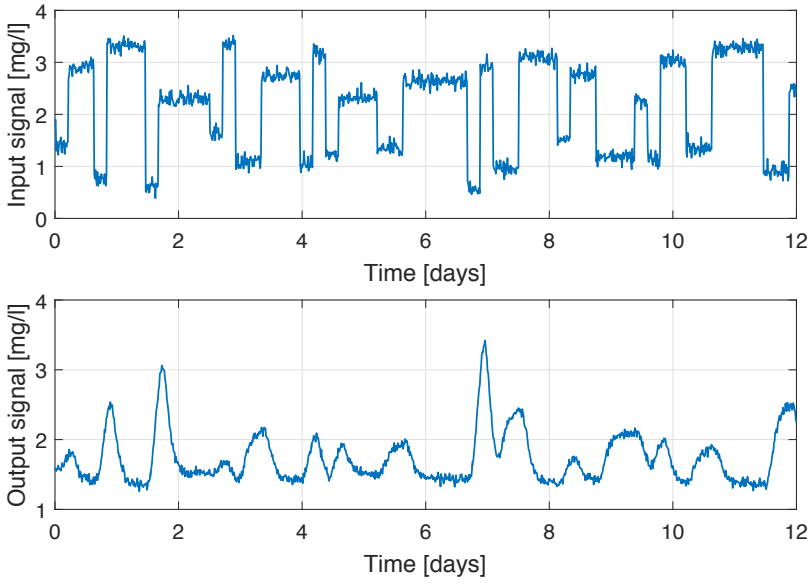

Figure 4: Simulated noisy data.

The generated signal is characterized by a mean, a certain amplitude and an interval length. The amplitude describes the maximum variation around the mean value. The interval length is the minimum duration of a certain input signal level. Due to system characteristics, the mean value is determined to be 2 g/m^3, which is the set point for DO, and hence the amplitude can not be higher than 2 g/m^3 to avoid negative values. The output signal, $y(t)$, is an effluent concentration level of ammonium NH_4. The noise that was added to the signal was a white noise process with standard deviation of 0.1 g/m^3 of the original signal.

For the numerical experiment, the plant was simulated twice using the simplified BSM1 and a constant influent flow. The simulation time was 12 days with 15 minutes sampling time. Two different input signal realizations

were tested in order to compare modelling performance for different input signals. The signal characteristics are given by Table 4.1.

Table 4.1: Simulated input signals

Signal	Min interval length	Max amplitude
1	20	1
2	20	1.5

The noise was added after simulations to both the input and the output signal, and was hence assumed to be a measured noise originating from sensors. An example of the generated input and output data sets used for identification is shown in Fig. 4.

4.2 Identification results

During the identification, several model orders and parameters were tested experimentally and the best obtained estimation models were used for a comparison. For the linear part of the Hammerstein identification methods, the polynomial orders for (3) and (4) were chosen to be $n_b = 7$ and $n_a = 6$ respectively for PEM model and $n_b = 6$ and $n_a = 7$ respectively for RPEM model. The time delay was set to $n_k = 6$ in both cases.

The performance was evaluated using validation data sets generated separately and the results are given as a fit of an estimated output to the simulated output in Table 4.2. Note that means were removed from both input and output signals for identification and then added back.

Table 4.2: Identification results

Model	Signal 1	Signal 2
Linear OE	52%	45%
PEM Hammerstein	72%	78.5%
RPEM Hammerstein	72%	78.4%

As shown by Table 4.2, the linear OE identification method has a poor performance for both signal sets, while the identified nonlinear Hammerstein models provide a more accurate prediction of output signals and handle the noise and amplitude variations well. The prediction results varied within a 70-80% fit, depending on signal properties and model orders. The results for the best performance, Signal 2, obtained by the Hammerstein models are discussed in more details below.

The identification results using Signal 2 are shown in Fig. 5. As can be seen in Fig. 5, both Hammerstein methods result in an accurate input-output description of the system. The modelling error is significant for the linear OE model. Fig. 6 shows the Bode plot of the linear block of the generated system.

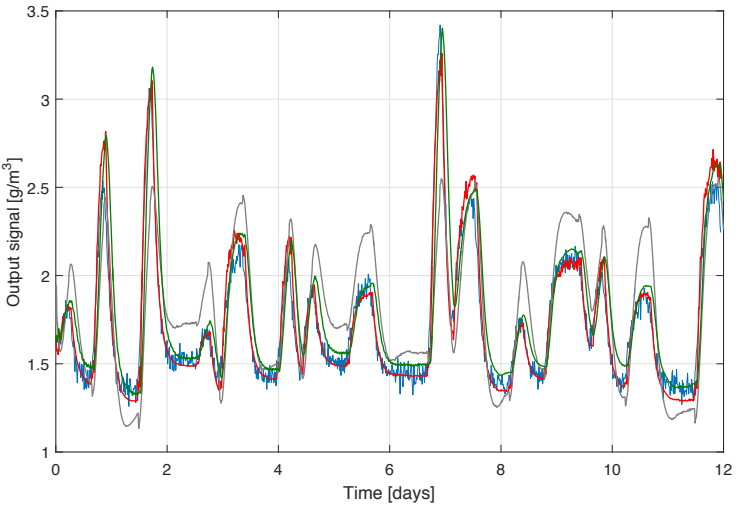

Figure 5: Signal 2. Validation results for linear OE method (grey), PEM Hammerstein method (green), RPEM Hammerstein method (red) and real data (blue).

The nonlinearities were parametrized by the following grid points

$$\begin{aligned}\mathcal{G}_{PEM} = [&-1.9 \quad -1.2 \quad -0.8 \quad -0.6 \quad -0.5 \\ &-0.2 \quad 0.5 \quad 0.51 \quad 0.8 \quad 1.2],\end{aligned} \tag{21}$$

$$\mathcal{G}_{RPEM} = [-1.7 \quad -0.99 \quad -0.25 \quad 0.25 \quad 0.9], \tag{22}$$

for the PEM and RPEM respectively. The grid points for the PEM method are automatically adapted by the MATLAB® function *nhlw* as mentioned in Section 3.2. The static nonlinearities identified by the algorithms are shown in Fig. 7 and 8. The behaviour of the identified nonlinearities are similar. In the case study, the decreasing static nonlinearity occurs since the Hammerstein methods are black-box methods. Therefore, when the operating point is increased, the differential gain of the underlying physical Monod function, see [6], is reduced which is reflected by the identified nonlinearity. This situation is different from the one in [6] where a Monod function is postulated as nonlinearity.

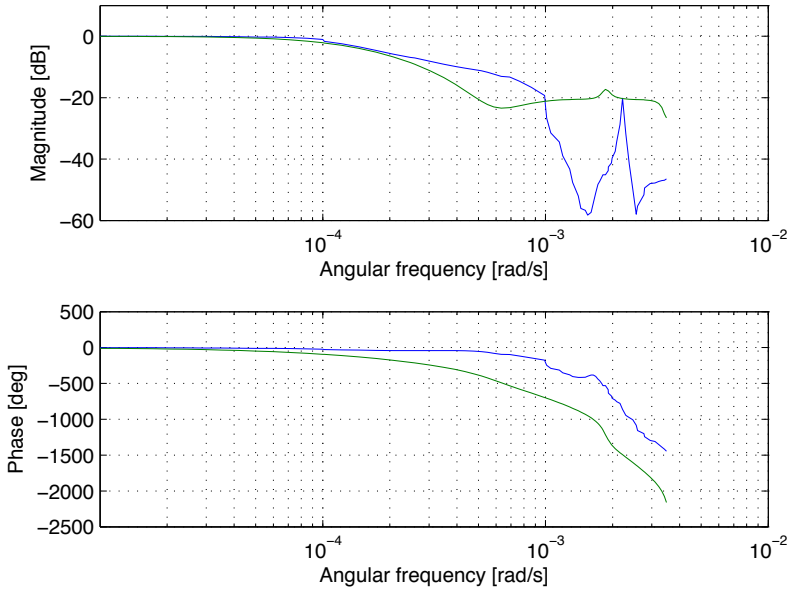

Figure 6: Signal 2. Bode plot of the linear part obtained with PEM (blue) and RPEM (green) Hammerstein models.

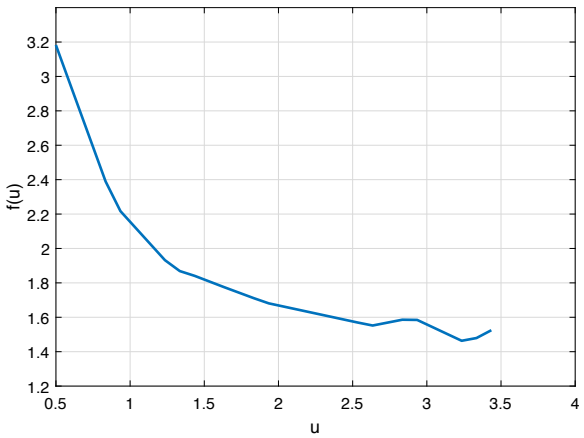

Figure 7: Signal 2. Static nonlinearity obtained with the PEM Hammerstein method.

The convergence of the parameter estimates for the RPEM are shown in Fig. 9. It can be concluded that the algorithm converges towards constant values in a well behaved manner.

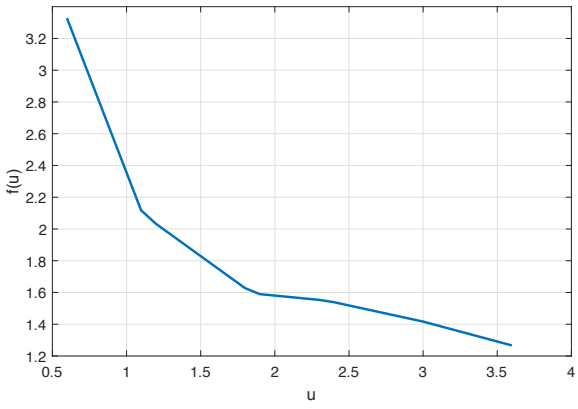

Figure 8: Signal 2. Static nonlinearity obtained with the RPEM Hammerstein method.

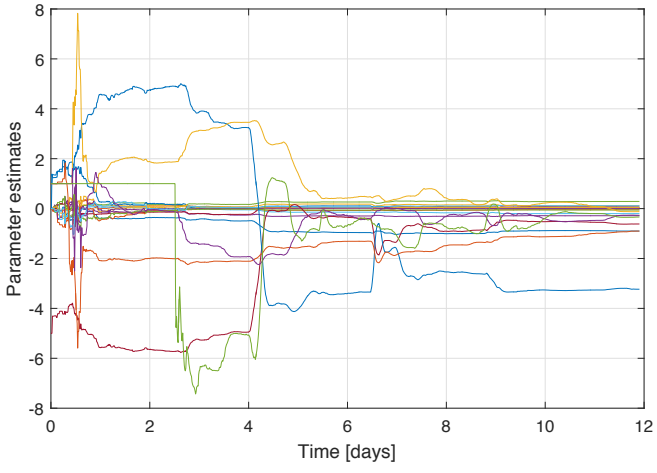

Figure 9: Signal 2. Parameter estimates obtained with the RPEM Hammerstein method.

In summary, the obtained results show that accurate identification of the nonlinear dynamics of the WWT plant can be obtained by application of Hammerstein identification techniques.

5. Conclusions

Three system identification methods have been compared: a linear output error method, a nonlinear Hammerstein identification algorithm of the MATLAB® System Identification Toolbox and a recursive prediction error Hammerstein model based algorithm.

The methods were used to identify the dissolved oxygen to effluent ammonia dynamics using noisy data from a simulated nitrifying bioreactor in a WWT plant model. The idea was to provide a simplified, but accurate, nonlinear Hammerstein model by application of system identification. This model reduction step, when successful, enables the design of an $\mathcal{L}_2$-stable feedback controller for the plant, this controller being described in a subsequent publication.

The results of the study indicates that a Hammerstein model can indeed describe the bioreactor dynamics with quite high accuracy. The output error method based on a linear model resulted in a significantly lower accuracy as compared to the nonlinear models. Of the two tested Hammerstein identification methods, the recursive method enjoys advantages for adaptive operation and on-line fault detection purposes.

Topics for further studies include a generalization of the identification to several cascaded reactors. The identified Hammerstein model will then be used as a basis for an $\mathcal{L}_2$-stable controller design.

Bibliography

[1] E. Abd-Elrady, "An adaptive grid point algorithm for harmonic signal modeling", *Proceedings of 15th IFAC World Congress on Automatic Control*, Barcelona, Spain, pp. 193-198, 2002.

[2] L. Åmand, "Ammonium feedback control in wastewater treatment plants", Ph.D. thesis, Uppsala University, Uppsala, Sweden, 2014. Available on-line at http://uu.diva-portal.org.

[3] K. J. Åström and R.D. Bell, "Drum-boiler dynamics", *Automatica*, vol. 36, no. 3, pp. 363-378, 2000.

[4] L. Breiman, "Hinging hyperplanes for regression, classification and function approximation", *IEEE Transactions on Information Theory*, vol. 39, no. 3, pp. 999-1013, 1993.

[5] L. Brus, "Nonlinear identification of a solar heating system", *Proceedings of 2005 IEEE Conference on Control Applications*, Toronto, ON, Canada, pp. 1491-1497, 2015.

[6] T. Chistiakova, T. Wigren, and B. Carlsson, "Input-Output Stability Design of an Ammonium Based Aeration Controller for Wastewater Treatment", *Manuscript submitted for publication.*.

[7] J. Alex, L. Benedetti, J. Copp, K.V. Gernaey, U. Jeppsson, I. Nopens, M.N. Pons, L. Rieger, C. Rosen, J.P. Steyer, *et al.*, "Benchmark Simulation Model No. 1 (BSM1)", Division of Industrial Electrical Engineering and Automation, Lund University, 2008

[8] M. Ekman, "Bilinear black-box identification and MPC of the activated sludge process", *J. Process Contr.*, vol. 18, no. 7, pp. 643-653, 2008.

[9] M. H. Gerardi, *Nitrification and Denitrification in the Activated Sludge Process.* New York, NY, USA: Wiley, 2003.

[10] F. Giri and E.-W. Bai, *Block-oriented nonlinear system identification.* Springer, London, UK, 2010.

[11] M. Henze, "Activated sludge model no. 1", *IAWPRC Scientific and Technical Reports*, 1, London, UK: IWA Publishing, 1987.

[12] J.-N. Lin and R. Unbehauen, "Canonical piecewise-linear approximations", *IEEE Transactions on Circuits and Systems I: Fundamental Theory and Applications*, vol. 39, no. 8, pp. 697-699, 1992.

[13] L. Ljung, *System Identification: Theory for the User*. Upper Saddle River, NJ, USA: Prentice Hall, 1999.

[14] L. Ljung, *System Identification Toolbox: Users Guide Version 7.4*. Natick, MA, USA: The Mathworks, 2011.

[15] P. Mattsson and T. Wigren, "Recursive identification of Hammerstein models", *Proc. 2014 American Control Conference*, Portland, Oregon, USA, pp. 179-186, 2014.

[16] P. Mattsson and T. Wigren, "Convergence analysis for recursive Hammerstein identification", *Automatica*, vol. 71(C), pp. 2498-2503, 2016.

[17] R. Pintelon and J. Schoukens, *System Identification: A Frequency Domain Approach*. Wiley, New Jersey, USA, 2012.

[18] T. Söderström and P. Stoica, *System identification*. Hemel Hempstead, UK: Prentice-Hall, 1989.

[19] S. Tayamon and T. Wigren, "Control of Selective Catalytic Reduction Systems Using Feedback Linearisation", *Asian Journal of Control*, vol. 18, no. 3, pp. 802-816, 2016.

[20] G. Olsson, M. Nielsen, Z. Yuan, A. Lynggaard-Jensen and J. Steyer, *Instrumentation, Control and Automation in Wastewater Systems*, London, UK: IWA Publishing, 2005.

[21] G. Olsson and B. Newell, *Wastewater Treatment Systems: Modeling, Diagnosis and Control*, London, UK: IWA Publishing, 1999.

[22] M. Vidyasagar, *Nonlinear Systems Analysis*. Englewood Cliffs, NJ, USA: Prentice-Hall, 1978.

[23] T. Wigren, "Recursive prediction error identification and scaling of non-linear state space models using a restricted black box parameterization", *Automatica*, vol. 42, no. 1, pp. 159-168, 2006.

[24] T. Wigren, "User choices and model validation in system identification using nonlinear Wiener models", *Proceedings of 13th IFAC Symposium on System Identification*, Rotterdam, The Netherlands, pp. 863-868, 2003.

[25] T. Wigren, "Nonlinear identification of neuron models", *Proc. IEEE CCA 2015*, Sydney, Australia, pp. 1340-1346, 2015.

[26] T. Wigren, "Low-frequency limitations in saturated and delayed networked control", *Proc. IEEE CCA 2015*, Manly, Sydney, NSW, Australia, pp. 564-571, 2015.

Paper II

Nonlinear modelling of the dissolved oxygen to ammonium dynamics in a nitrifying activated sludge process

Tatiana Chistiakova, Bengt Carlsson and Torbjörn Wigren [1]

Abstract

Modelling of the activated sludge process is, for example, important for controller design and stability analysis. The paper presents a comparison of several identification methods based on data from a simplified version of the Benchmark Simulation Model no. 1. The goal is to find accurate dynamic models on how the effluent ammonia in a nitrifying activated sludge process depends on the dissolved oxygen concentration and on the influent load. The tested models include a linear one and several variants of Hammerstein models. The models are estimated using noisy data and measured disturbances. Due to the high complexity and nonlinear character of the system, the nonlinear models perform better than the linear one.

[1]Department of Information Technology, Uppsala University, SE 75105 Uppsala, Sweden

1. Introduction

The aeration of biological reactors in an activated sludge process (ASP) is normally the most energy demanding process in wastewater treatment plants (WWTPs), [2]. Automatic control of the aeration is hence of fundamental importance to achieve an energy efficient operation. Supervisory ammonium feedback control, [1], is a control strategy that today is becoming more and more common in full-scale plants. In its basic form, this strategy uses feedback from effluent ammonium to select the set points for all dissolved oxygen (DO) controllers in the aerated zones.

The aim of the presented work is to develop simple but accurate nonlinear models of the dissolved oxygen to ammonium dynamics using a static nonlinear model followed by a linear model, i.e. a Hammerstein model, [6]. This is of interest for several reasons. It could (i) improve the control performance by using exact linearisation (i.e. using the inverse of the estimated static nonlinearity after a standard linear controller) and (ii) be used to perform a stability analysis of the closed loop system by using the Popov criterion, [8], as is done in [4]. The model itself may also be used for model based monitoring and fault detection. The Hammerstein models of the present paper include also grey-box models, as compared to the black-box models studied in the related work, [3].

2. Simulation Model

Data from a simplified version of the Benchmark Simulation Model no. 1 (BSM1), [5], was used for system identification, i.e. calibration, of the parameters in the models using input-output data. The model consists of one biological reactor followed by a clarifier, see Fig. 1. The volume of the reactor was 3999 m^3.

The DO set-point was used as an input signal, $u(t)$, to the simulation model. The output signal was the effluent ammonium concentration, $y(t)$. White noise with a standard deviation of 0.1 mg/l was added to the output signal. The sampling period was 15 minutes.

Two cases were studied. The first case was defined by constant influent data using two data sets for model calibration: 12 days (1154 samples) and 2 days (200 samples). An example of data used for calibration in the first case is shown in Fig. 2. In this case, $Q_{in} = 18446\ m^3/day$, $NH_{4,in} = 31.5\ mg/l$, $RAS = Q_{in}$ and WAS was selected so that the sludge retention time was 4 days.

In the second case, time-varying influent data was used. The influent flow rate Q_{in} and influent ammonium concentration $NH_{4,in}$ from the original BSM1 influent files were scaled down by a factor of 0.3 in order to give a

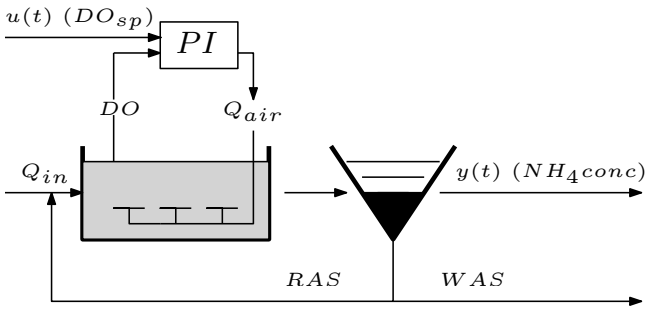

Figure 1: Simulation model. Q_{in}-inflow, $u(t)$-input signal (DO_{sp}-DO set point), PI-proportional integral DO controller, Q_{air}-airflow rate, $y(t)$-output signal (NH_4conc-ammonium concentration), RAS-return activated sludge, WAS-waste activated sludge.

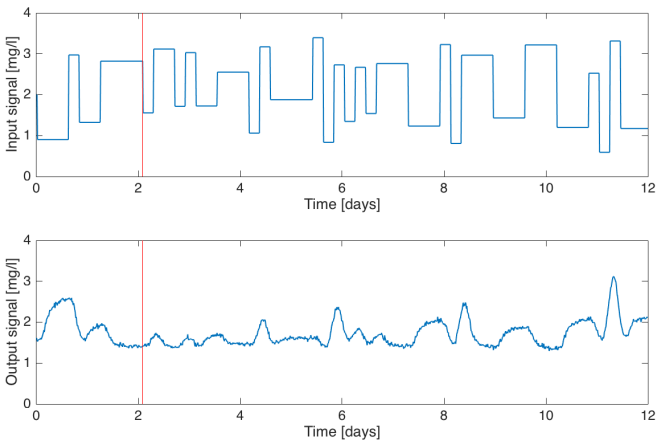

Figure 2: Example of a simulated data realization. The red line shows the end of the short experiment. Constant influent case.

reasonable disturbance pattern given the chosen volume of the bioreactor. The influent data for the time-varying case are shown in Fig. 3. A data set with 1154 samples was used in this case.

For the second case, an additional input signal was used in the modelling, given as

$$w(t) = Q_{in}(t) \cdot NH_{4,in}(t), \tag{1}$$

where Q_{in} is the inflow rate and $NH_{4,in}$ is the influent ammonium concentration. Then, the basic model structure used for system identification

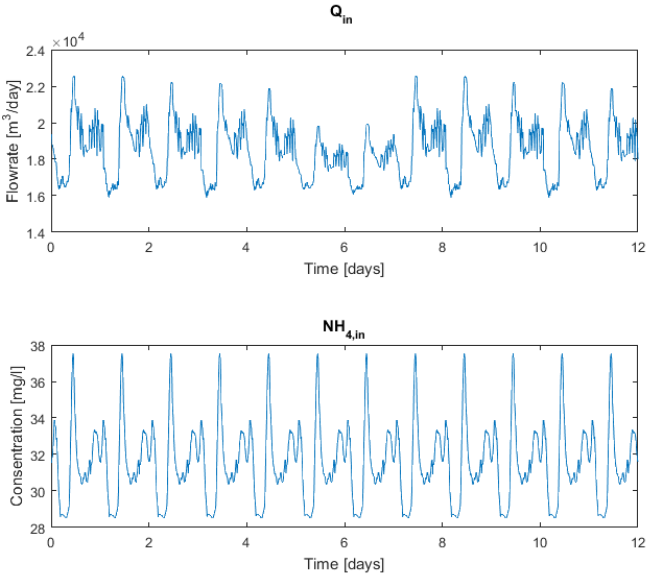

Figure 3: Inflow rate Q_{in} and influent ammonium concentration $NH_{4,in}$. Time-varying influent case.

is given by

$$y(t) = H_1(q^{-1})u(t) + H_2(q^{-1})w(t), \tag{2}$$

where $y(t)$ is the output signal (effluent ammonium concentration), $u(t)$ is the input signal (DO set point) and $w(t)$ is the measured disturbance used as input to the disturbance model. The operators $H_1(q^{-1})$ and $H_2(q^{-1})$ is in the linear case ordinary discrete time transfer function operators.

3. Methods

3.1 Linear Output Error Model

As a reference case, a linear output error model (LOE) was used. The LOE is described by a linear transfer function as

$$\hat{y}(t) = \frac{B(q^{-1})}{A(q^{-1})}u(t), \tag{3}$$

where

$$B(q^{-1}) = b_1 q^{-n_k} + ... + b_{n_b} q^{-n_k - n_b + 1}, \tag{4}$$

$$A(q^{-1}) = 1 + a_1 q^{-1} + ... + a_{n_a} q^{-n_a} \tag{5}$$

are polynomials in the backward shift operator q^{-1} and n_k is the time delay (dead time). The $MATLAB^{TM}$ function *oe* was applied for estimation of the parameters. See [7] for a detailed explanation.

Using extensive numerical experiments, it was found that a reasonable model order for the LOE is $n_a = 4$, $n_b = 3$ with a time delay of $n_k = 5$. These model orders were also used in the linear part of all nonlinear models described below as well as in the $H_2(q^{-1})$ in (2) describing the measured disturbance for the time-varying case.

3.2 Standard Hammerstein Model

A basic nonlinear model is the Hammerstein model defined in Fig. 4.

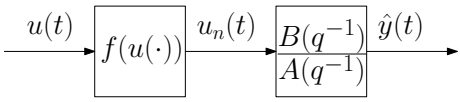

Figure 4: A Hammerstein model consisting of a nonlinear static function followed by a linear discrete model.

The linear block is described by (3). The nonlinearity in the standard Hammerstein case was chosen as a piecewise linear function and defined as

$$u_n(t, \theta_n) = f(u(t), \theta_n), \tag{6}$$

where θ_n is a vector containing the nonlinear parameters. See [3] for details of such piecewise linear parametrizations. The model is denoted SHAM, and it is estimated by the $MATLAB^{TM}$ function *nlhw*, [7].

3.3 Single Monod Hammerstein Model

As a way to obtain a static nonlinear model with fewer parameters than SHAM, a single Monod function was used as static nonlinearity. This model is denoted SMHAM and it is defined by the linear model (3) together with the Monod function

$$u_n(t) = \mu_{max} \frac{u(t)}{u(t) + k_o}, \tag{7}$$

where μ_{max} is the maximum growth rate and k_o is the half saturation constant for dissolved oxygen. The model calibration was performed using a grid search for k_o. For each value of k_o, a new transformed input signal $u_n(t)$

was calculated and used as input to the LOE model. The $MATLAB^{TM}$ function *oe* was then applied to obtain the linear parameters.

In the model, $\mu_{max} = 0.5$ was used, this value is, however, not critical since deviation from this gain factor is implicitly modelled by the linear part.

3.4 Double Monod Hammerstein Model

Finally, a double Monod model, denoted DMHAM, was used as a nonlinear model. This model is given by (3) together with

$$u_n(t) = \mu_{max} \frac{u(t)}{(u(t) + k_o)} \frac{y(t - n_k)}{(y(t - n_k) + k_{NH_4})}, \tag{8}$$

where $n_k = 5$ is the number of delayed samples and k_{NH_4} is the half saturation constant for ammonium. The use of a delayed ammonium concentration $y(t - n_k)$ instead of $y(t)$ gave a better model performance and was therefore chosen. The estimation of the parameters was done in the same way as for SMHAM except that a two-dimensional grid search for k_o and k_{NH_4} was used. For each two-dimensional grid point a new transformed signal $u_n(t)$ was calculated and used as input for the LOE model (3). The $MATLAB^{TM}$ function *oe* was then applied to identify the parameters of (3). Note that DMHAM is strictly speaking not a Hammerstein model since the nonlinear function does not depend on the input only.

SMHAM and DMHAM may be classified as grey-box models (or semi physical models), [6], since part of the model structure is obtained from process knowledge. Due to the grid search, standard tools like the $MATLAB^{TM}$ function *oe* can be reused for estimating the linear part of the model.

4. Results

4.1 Performance Criterion

The model parameters were estimated i times using i realizations of input-output data from the simplified BSM1 ($i = 100$ for the constant influent case and $i = 50$ for the time-varying influent case). In each of the trials, a second data set ("validation data") was used to compare the models ability of reproducing a new data set.

The models were evaluated using a measure of fit, the normalized root mean square error fitness value. The fit is given in percent and defined as

$$fit = 100 \cdot \left(1 - \frac{||y - \hat{y}||}{||y - \bar{y}||}\right), \tag{9}$$

where y is the output in the validation data, $\hat{y}$ is the simulated output produced by the estimated model and $\bar{y}$ is the mean value of the validation output data.

4.2 Constant Influent Case

The goodness of fit produced by the different models is shown in Fig. 5 (long experiment) and Fig.6 (short experiment). For the long experiment, the flexible SHAM gave the best fit with a median value of the fit close to 90%. All nonlinear models gave a significantly better fit than the linear model (LOE). For the short experiment, the spread increased as expected. For this case, DMHAM gave the best results closely followed by SHAM.

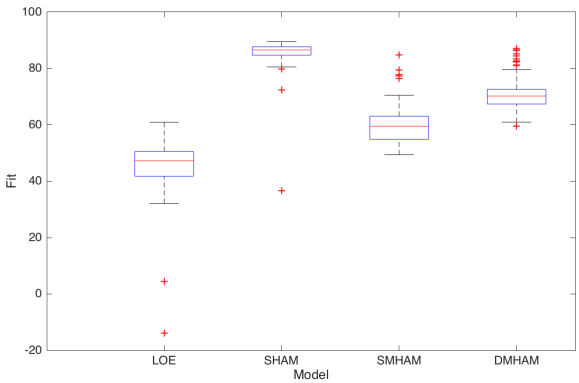

Figure 5: Boxplot (see *help boxplot* in $MATLAB^{TM}$) of goodness of fit for 100 trials, long experiment (1154 samples). Constant influent case.

The study indicates that SHAM and DMHAM are the best models for describing the dissolved oxygen to effluent ammonium dynamics. For stability analysis SHAM or SMHAM are recommended, since based on Chistiakova et al. (2017b) the Popov criterion is not valid for DMHAM.

4.3 Time-varying Influent Case

As a brief initial study, two models, LOE and SMHAM, were identified in the time-varying influent case. The results show that the nonlinear model is still a better choice to describe the system dynamics. Fig.7 shows a boxplot of the goodness of fit for the time-varying influent case. The median fit obtained was 36% for LOE model and 45% for SMHAM. The simulated output data obtained for the two models that provided the maximum fit are plotted against the validation data in Fig.8.

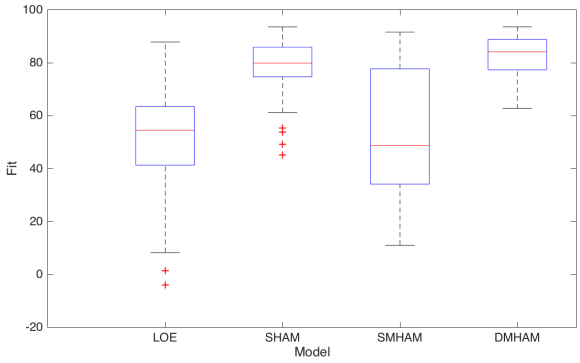

Figure 6: Boxplot of goodness of fit for 100 trials, short experiment (200 samples). Constant influent case.

To describe the result of the identification, Fig. 9 and Fig. 10 display the Bode plots of the identified transfer functions $H_1(q^{-1})$ and $H_2(q^{-1})$ of (2). In addition, Fig.11 illustrates the estimated static nonlinearity in (7).

5. Conclusions

Simple nonlinear dynamic models, estimated from input-output data, could fairly well describe the effluent ammonium concentration in a simulated nitrifying activated sludge process. The simplicity of the models make them ideal for controller design (e.g. exact linearization) and stability analysis of an ammonium feedback control system. Future research will, however, first be focused on a more detailed modelling study for the time-varying influent case (which indeed is the practically most relevant scenario). Such a study should consider at least the same models as in the time-invariant case of the current paper. It might also be of interest to investigate if a nonlinear model of the disturbances would improve the model fit.

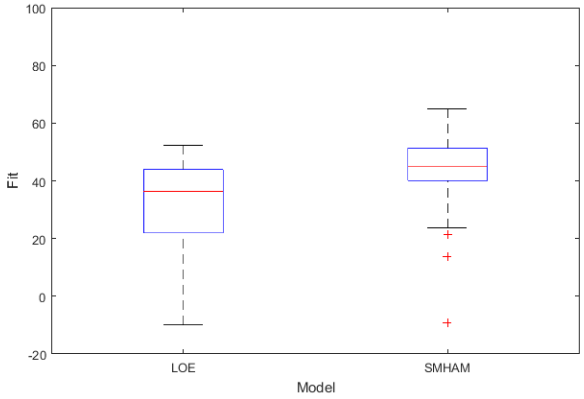

Figure 7: Boxplot of goodness of fit for 50 trials, long experiment (1154 samples). Time-varying influent case.

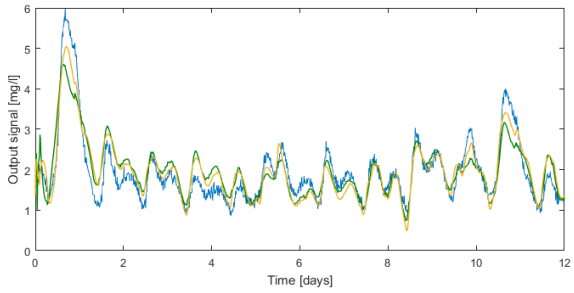

Figure 8: Example of output data. Blue line - validation data set, yellow line - estimation by SMHAM model, green line - estimation by LOE model. Time-varying influent case.

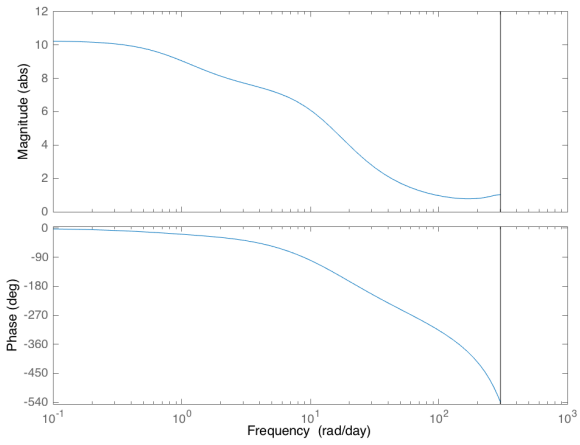

Figure 9: Bode plot for H_1 of the linear part obtained with SMHAM model, the black line is Nyquist frequency. Time-varying influent case.

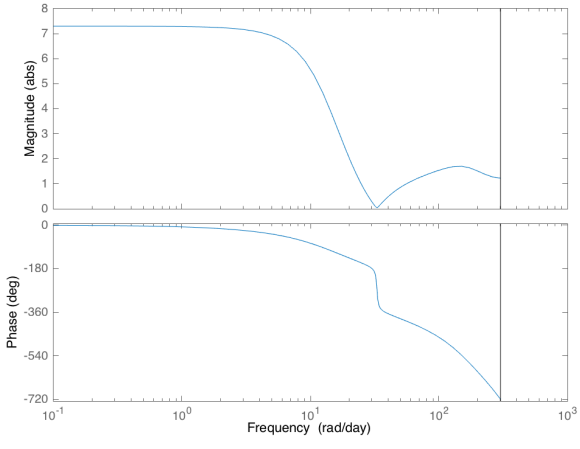

Figure 10: Bode plot for H_2 of the linear part obtained with SMHAM model, the black line is Nyquist frequency. Time-varying influent case.

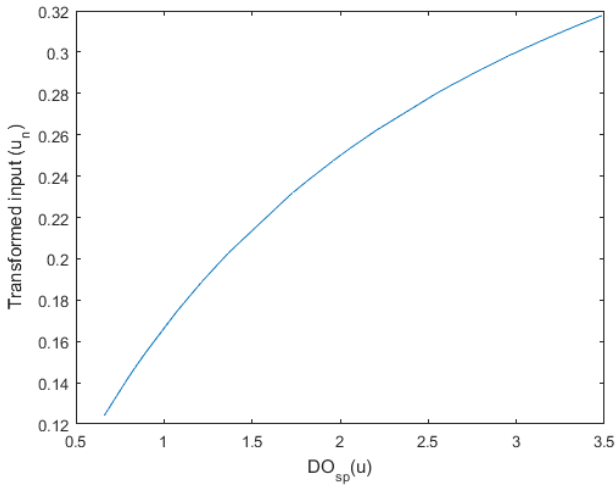

Figure 11: Static nonlinearity of the system obtained with SMHAM model. Time-varying influent case.

Bibliography

[1] L. Åmand, "Ammonium feedback control in wastewater treatment plants", Ph.D. thesis, Uppsala University, Uppsala, Sweden, 2014. Available on-line at http://uu.diva-portal.org.

[2] L. Åmand, G. Olsson and B. Carlsson, "Aeration control - a review", *Water Science and Technology*, vol. 67(11), pp. 2374-2398, 2013.

[3] T. Chistiakova, P. Mattsson, B. Carlsson and T. Wigren, "Nonlinear system identification of the dissolved oxygen to effluent ammonia dynamics in an activated sludge process", *Proc. IFAC 2017 World Congress*, Tolouse, France, pp. 3978-3983, July 9-15, 2017.

[4] T. Chistiakova, T. Wigren, and B. Carlsson, "Input-Output Stability Design of an Ammonium Based Aeration Controller for Wastewater Treatment", *submitted for publication.*

[5] K. Gernaey, U. Jeppsson, P. Vanrolleghem and J. Copp J, "Benchmarking of Control Strategies for Wastewater Treatment Plants", Scientific and Technical Report No. 23, IWA publishing, 2014.

[6] L. Ljung, *System Identification: Theory for the User.* Upper Saddle River, NJ, USA: Prentice Hall, 1999.

[7] L. Ljung, *System Identification Toolbox: Users Guide Version 7.4.* Natick, MA, USA: The Mathworks, 2011.

[8] M. Vidyasagar, *Nonlinear Systems Analysis.* Englewood Cliffs, NJ, USA: Prentice-Hall, 1978.

Paper III

Input-Output Stability Design of an Ammonium Based Aeration Controller for Wastewater Treatment

Tatiana Chistiakova, Torbjörn Wigren and Bengt Carlsson [1]

Abstract

Ammonium feedback is commonly used for controlling the aeration in wastewater treatment plants having biological nitrogen removal. The paper proposes the use of a PI controller tuning method based on a simplified identified model with Hammerstein structure. The Hammerstein model accounts for the delay of the process caused by the settler, the multiple bioreactors dynamics and the main nonlinear process effects. The controller tuning method exploits the Popov inequality for a precomputation of (a subset of) the stability region of the closed loop system as a function of the PI-controller parameters, quantified in terms of the maximum loop delay of the system. The controller parameters are selected in the computed stability region. In the numerical study, the plant is identified as a Hammerstein model using a recently published method, here extended to identify multiple bioreactor tank dynamics. The identification data is obtained from a high fidelity simulator, which is also used for evaluation of the proposed controller tuning method. The results show that the proposed procedure results in a PI-controller tuning with predictable stability properties and a good performance.

[1]Department of Information Technology, Uppsala University, SE 75105 Uppsala, Sweden

1. Introduction

The supply of clean water is an increasing matter of concern in many parts of the world. Cost effective wastewater treatment is therefore of fundamental importance, [1]. The most energy consuming process in a wastewater treatment plant is the aeration of wastewater, which is needed to remove nitrogen and organic carbon using the commonly applied activated sludge process (ASP), [2]. Ammonium feedback control is an increasingly popular strategy in ASPs designed for nitrification, see e.g. [3] and [4]. This control technique uses measurements of the ammonium concentration in the effluent water, or in the last reactor, to calculate the set point for the dissolved oxygen (DO) concentration for all local DO controllers, one in each of the aerated zones. A large amount of techniques and model configurations are available for modelling and simulation of wastewater treatment plants based on a variety of priorities and benefits, [5]. However, the majority of models rely on the state of the art model, created by an International Water Association (IWA) task group in 1983. This model is known as the Activated Sludge Model no.1 (ASM1). The model represents the process dynamics with 13 process variables, 19 model parameters and 8 process equations, [6].

The high order and nonlinear character of the ASM1 model makes it challenging to use it as a basis for controller design. The first contribution of the paper therefore attempts to find a simplified but still accurate model of the DO to effluent ammonium dynamics. The model is selected to have a Hammerstein structure with a static nonlinear input function. An increasing DO concentration level leads to a decrease in the ammonium, however, it also causes a decrease in the relative efficiency of the DO set point control system. This effect is incorporated in the static nonlinearity of the Hammerstein model, see [7]. In the closed loop system, a second nonlinearity appears due to limitations of the maximum and mimimum levels of the ammonium controller. The reason is that a too low DO level (for example, less than 1 g/m^3) may give negative process effects like unwanted N_2O emissions, [8], and a too high DO level (for example, more than 3 g/m^3) gives a high energy consumption with little effect on the effluent ammonium concentration. Another aspect of the paper is to identify a time delay to account for the lag between the DO and the effluent ammonium. The delay, which is caused by the settler, is integrated with the linear dynamics of the Hammerstein model, that represents the nonlinear biological and hydraulic dynamics of the three wastewater bioreactors. An identification algorithm, extended from the single bioreactor application of [7], is used for identification. The presence of limitations and a significant delay in the control loop means that it is relevant to account for the low frequency gain of the loop, as in [9] and [10]. Following [10], a pre-computation of a projection

of a subset of the $\mathcal{L}_2$ stability region of the loop formed by the identified Hammerstein model is then performed, based on the Popov inequality [9]. The reason for the subset is that the Popov criterion is not necessary for stability. The projection of the subset of the stability region is computed as a function of a selected set of controller parameters. Given the stability region, an $\mathcal{L}_2$-stable controller is selected, with specified stability robustness against, for example, a selected range of delays. Provided that the identified Hammerstein model is accurate enough, stability robustness should then carry over to the control loop for the complete simulation model. This procedure, applied to wastewater treatment, constitutes another contribution of the paper. Finally, a numerical study is used to illustrate the design procedure and the performance of the resulting controller.

Previous work related to the present paper include the general work on wastewater treatment of e.g. [2], [11] and [12]. The underlying processes relevant for the present paper are outlined further in e.g. [6], [8] and [13]. There is a large amount of system identification methods tailored for Hammerstein systems available in the literature, see e.g. [14] for a review and further details. A variety of these methods are nowadays ready for use in commercially available software packages, like [15]. The previous work of the authors on the ammonium control problem has recently been focused on Hammerstein identification of plants with a single reactor. The recursive Hammerstein identification method of [16] was e.g. applied in [17], while the grey-box method applied in the present paper was introduced in [7]. Since the ammonium control system is nonlinear with constraints, nonlinear methods for control like model predictive control (MPC), [18], are generally applicable. However, MPC is complex, with complicated stability conditions, which is a reason why more simple methods constitute interesting alternatives, c.f. e.g. [8] and [19]. It is finally noted that the idea to precompute the stability region is inspired by the wireless network data flow control problem outlined in [9], [10], and the references therein.

The organization of the paper is as follows. The activated sludge process is reviewed in Section 2, followed by a description of the system identification method in Section 3. The ammonium control system of the paper is discussed in Section 4, with the key stability aspects detailed in Section 5. A numerical study and conclusions end the paper in Sections 6 and 7.

2. The Activated Sludge Process

Wastewater treatment plants usually consist of a number of process steps including mechanical, biological and chemical treatments. After the mechanical treatment, where most particulate matter is removed, the wastewater

enters the biological treatment process where nitrogen is removed in an ASP.

The process of nitrification involves microorganism activity and requires a supply of DO in order to convert ammonium to nitrate. Hence, nitrification occurs in aerobic compartments of bioreactors where the DO concentration is kept at a certain level high enough to keep a required removal rate. A standard control approach is to maintain the DO concentration level at a fixed point, [12]. However, such a strategy might result in an increased energy consumption together with a decreased flexibility of the system. An ammonium feedback control system on the other hand allows the DO set point to be regulated which improves the system performance, [8].

Fig. 1 shows a schematic representation of an ASP with three aerated zones and a settler. The DO set point is controlled by a PI ammonium (NH_4) based controller with leakage, see Section 4.2.

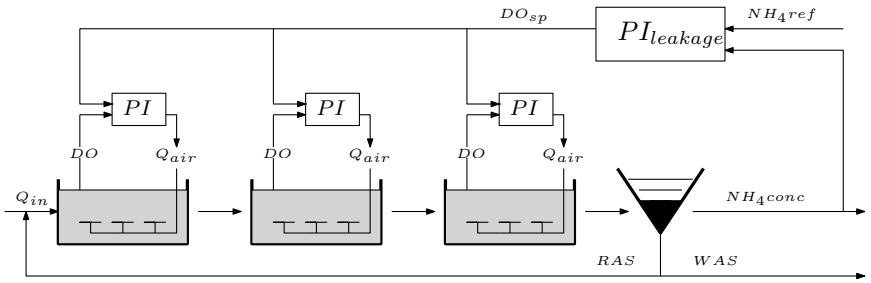

Figure 1: Control structure in the simulation model. Q_{in}-inflow, DO_{sp}-DO set point, PI-proportional integral controller, $PI_{leakage}$-DO_{sp} proportional integral controller with leakage, Q_{air}-airflow rate, NH_4conc-ammonium concentration, NH_4ref - ammonium reference value, RAS-return activated sludge, WAS-waste activated sludge.

Apart from the nonlinear dynamics, the ammonium controller has upper and lower saturation limits on the control signal DO_{sp}. In this study, the $DO_{sp_{min}} = 1$ g/m^3 and $DO_{sp_{max}} = 3$ g/m^3.

The high fidelity model used in the paper is based on Benchmark Simulation Model no.1 (BSM1), [13], implemented in $MATLAB^{TM}/Simulink^{TM}$, which defines a plant layout and allows simulations and testing under realistic conditions. To pinpoint the aeration control problem, the anoxic zones where denitrification takes place were omitted. Anoxic models could easily be added to the system (c.f. BSM1) without changing the basic problem set-up and the proposed solution.

The time delay is an important issue to consider when studying the ammonium control problem. In general, the delay is caused by the settler. In the case study, the delay occurs when the ammonium concentration is measured after the settler. This is a main aspect of the paper.

3. Identification method

3.1. The Monod Hammerstein model

The ASP dynamics is a highly nonlinear process with nonlinearitites originating from different sources including concentration saturation, growth rate dynamics and physical characteristics. This could results in a highly complicated controller. Hence, it is desirable to describe the system in a simple but still accurate way to simplify the controller design process.

In the case study, the nonlinearity of the process is described using a static Monod function, [20]. This technique gives a static nonlinearity with fewer parameters than, for example, a standard black-box Hammerstein model, like [16]. The nonlinearity of the process is thus modelled as

$$u(t) = \mu_{max} \frac{\bar{u}(t)}{\bar{u}(t) + k_o}, \tag{1}$$

where $\bar{u}(t)$ is the DO set point, μ_{max} is the maximum growth rate set to the constant value 0.5 and k_o is the half saturation constant, [13].

The linear part of the Hammerstein model is given by

$$\hat{y}(t) = \frac{B^d(q)}{A^d(q)} u(t), \tag{2}$$

where $B^d(q)$ and $A^d(q)$ are given by the filter polynomials

$$B^d(q) = b_1 q^{-n_k} + ... + b_{n_b} q^{-n_k - n_b + 1}, \tag{3}$$

$$A^d(q) = 1 + a_1 q^{-1} + ... + a_{n_a} q^{-n_a}, \tag{4}$$

where q^{-1} is the backward shift operator, n_a and n_b are the orders, and n_k is a delay quantified in terms of the number of samples, [21]. Typically, the delay represents the effect of the settler. The superscript d is used to emphasise that the polynomials are defined for a discrete-time model.

3.2. Identification algorithm

The Monod function parameter, k_o, was determined by gridding using an outer optimization loop. At each grid point, the Monod function was then used to compute the input signal to be used by the linear output error method of the $MATLAB^{TM}$ System Identification toolbox. The saturation constant that gave the best fit to the data defines the result of the Hammerstein system identification procedure together with the obtained linear parameters.

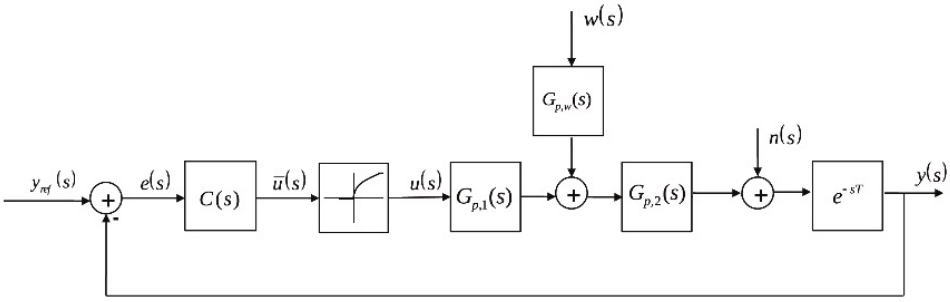

Figure 2: Block diagram of the ammonium control loop. The fact that $n(s)$ is added before e^{-sT} is to avoid theoretical problems with non-causality.

The identification of the linear system dynamics was performed using the standard $MATLAB^{TM}$ function *oe* for identification with the Output Error (OE) algorithm, see [15] for more details.

4. Model of the ammonium control loop

4.1. Controller

The complete ammonium control loop model can be described by the block diagram of Fig. 2. A continuous time formulation is used for controller design and analysis, assuming an identified discrete time system converted to continuous time according to zero-order-hold (ZoH) sampling conventions, [22]. Hence t denotes time and s is the Laplace transform variable. The ammonium reference value is denoted $y_{ref}(s)$. Together with the output signal $y(s)$ the control error of the single degree of freedom controller becomes

$$e(s) = y_{ref}(s) - y(s). \tag{5}$$

The controlled signal is governed by a controller as

$$\bar{u}(s) = C(s)e(s) = \left(K_P + K_I \frac{1}{s+\alpha}\right) e(s), \tag{6}$$

where $C(s)$ is chosen as a leaky PI controller with K_P being a proportional gain, K_I an integral gain and α a leakage variable. The selection of a PI controller structure is motivated by its widespread use in wastewater treatment plants, by its simplicity, and since operators are familiar with its behaviour. The leakage of the integral term is intended to limit the low frequency loop gain from above, and the sensitivity function from below. The reason is that the controller parameters, K_P, K_I and α, will later be

selected to be within a subset of the $\mathcal{L}_2$-stability region as defined by the Popov criterion, [23], and the Popov criterion does not allow open loop integration together with a saturation. In addition to this, Theorem 3 of [10] shows that a large delay, a saturation and a high low frequency loop gain is not consistent with $\mathcal{L}_2$-stability.

4.2. Plant dynamics and nonlinearities

The signal $\bar{u}(s)$ is the unrestricted control signal. However, $\bar{u}(s)$ is limited before being used as set points for the three DO controllers, see Fig. 1. Since the process is modelled by a Hammerstein model, the limitation (or saturation) can be cascaded with the identified Monod function. This static transformation is defined in the time domain. The complete static nonlinearity of the loop is hence given by

$$u(t) = \Phi(\bar{u}(t))$$

$$= \begin{cases} \varphi(\bar{u}_{min}), & \bar{u}(t) \leq \bar{u}_{min} \\ \varphi(\bar{u}(t)), & \bar{u}_{min} < \bar{u}(t) < \bar{u}_{max} \\ \varphi(\bar{u}_{max}), & \bar{u}(t) \geq \bar{u}_{max} \end{cases}, \tag{7}$$

where

$$\varphi(\bar{u}(t)) = \frac{\mu_{max}\bar{u}(t)}{\bar{u}(t) + k_o} \tag{8}$$

is the Monod function and the parameter k_o is obtained from the identification of the Hammerstein model of Section 3. The lower and upper limits $\bar{u}_{min}$ and $\bar{u}_{max}$ are selected manually.

The signal $u(s)$ then acts on the linear plant dynamics, as represented by the two transfer functions $G_{p,1}(s)$ and $G_{p,2}(s)$. These transfer functions are obtained by transformation of identified Hammerstein model of Section 3, for signal levels at a typical operating point. The disturbance $w(s)$ models variations in the influent wastewater that affects the output ammonium concentration. For generality, the transfer function $G_{p,w}(s)$ acts on $w(s)$ before the disturbance enters the plant in-between $G_{p,1}(s)$ and $G_{p,2}(s)$, thereby allowing parts of the dynamics to be shared between $u(s)$ and $w(s)$. The transfer functions of the feedback loop are assumed to be parameterized as follows:

$$G_{p,1}(s) = G_p \frac{(s + b_{1,1})...(s + b_{1,nb_1})}{(s + a_{1,1})...(s + a_{1,na_1})}, \tag{9}$$

$$G_{p,2}(s) = \frac{(s + b_{2,2})...(s + b_{2,nb_2})}{(s + a_{2,2})...(s + a_{2,na_2})}. \tag{10}$$

Here, $b_{1,i}$, $i = 1, ..., nb_1$, $a_{1,i}$, $i = 1, ..., na_1$ are the zeros and poles of $G_{p,1}(s)$, and $b_{2,i}$, $i = 1, ..., nb_2$, $a_{2,i}$, $i = 1, ..., na_2$ are the zeros and poles of $G_{p,2}(s)$.

Complex zeros and poles are assumed to appear as complex conjugate pairs and G_p denotes a static gain. Additive measurement noise $n(s)$ is added to give the output ammonium concentration $y(s)$. Finally, the delay effect of the settler is modelled as e^{-sT}, and it is also obtained by identification.

5. $\mathcal{L}_2$-stability conditions

As stated in the introduction, the intention is to pre-compute a subset of the $\mathcal{L}_2$-stability region and to use this region for selection of controller parameters, as in e.g. [10]. The formulation of the design algorithm first requires that the Popov criterion is stated.

5.1. The Popov criterion

Because of the delay, the infinite dimensional input-output stability version of the Popov criterion needs to be applied. The following definitions of [23] are needed to state the Popov criterion:

Definition 1: For all $p \in [1, \infty)$, $\mathcal{L}_p[0, \infty)$ denotes the set of all measurable functions $f(\cdot) : [0, \infty) \to R$, such that

$$\|f(\cdot)\|_p^p = \int_0^\infty |f(t)|^p dt < \infty.$$

Definition 2: The set of all measurable functions $f(\cdot) : [0, \infty) \to R$, such that their truncations

$$f_T(t) = \begin{cases} f(t), & 0 \le t \le T \\ 0, & t > T \end{cases} \in \mathcal{L}_p[0, \infty),$$

$\forall T$, is denoted the extension $\mathcal{L}_{pe}[0, \infty)$ of $\mathcal{L}_p[0, \infty)$.

Definition 3: The mapping $A : \mathcal{L}_{pe} \to \mathcal{L}_{pe}$ is $\mathcal{L}_p$-stable if i) $Af \in \mathcal{L}_p$ whenever $f \in \mathcal{L}_p$, and ii) there exist finite constants k and c, such that

$$\|Af\|_p \le k\|f\|_p + c, \quad \forall f \in \mathcal{L}_p.$$

Definition 4: $\mathcal{A}$ denotes the set of generalized functions of the form

$$f(t) = \begin{cases} 0, & t < 0 \\ \sum_{i=0}^\infty f_i \delta(t - t_i) + f_a(t), & t \ge 0, \end{cases}$$

where $\delta(\cdot)$ is the unit delta distribution, t_i are non-negative constant delays, $f_a(t)$ is measurable and

$$\sum_{i=0}^\infty |f_i| < \infty, \qquad \int_0^\infty |f_a(t)| dt < \infty.$$

Definition 5: $\hat{\mathcal{A}}$ denotes the set of all function $\hat{f} : C_+ \to C$ that are Laplace transforms of elements of $\mathcal{A}$.

The Popov criterion then follows:

Lemma 1: (Popov Criterion, [23] Theorem 6.7.63). Consider the system of Fig. 3. Assume that the inverse Laplace transform of the transfer function $\hat{g}(s)$ fulfils

$$g(\cdot) \in \mathcal{A}, \quad \dot{g}(\cdot) \in \mathcal{A},$$

that the time invariant static nonlinearity $\Phi(\cdot)$ fulfils

$$0 \leq \sigma\Phi(\sigma) \leq k\sigma^2,$$

and that $u_1 \in \mathcal{L}_2$, $u_2 \in \mathcal{L}_2$, $\dot{u}_2 \in \mathcal{L}_2$. Under these conditions the system is $\mathcal{L}_2$-stable if there exist constants q, δ, such that the Popov plot

$$\omega \in [0, \infty) \to Re[\hat{g}(j\omega)] + j\omega Im[\hat{g}(j\omega)] \in C$$

lies entirely to the right of a line through $-1/k + \delta + j0$ with slope $1/q$, for some $q \geq 0$ and some $\delta > 0$.

Proof: See [23], Section 6.7.

The subset of the $\mathcal{L}_2$-stability region is hence defined by the following Popov inequality

$$Re[(1 + j\omega q)\hat{g}(j\omega)] + \frac{1}{k} \geq \delta > 0, \ \forall\omega \geq 0, \text{some } q > 0. \tag{11}$$

5.2. Ammonium control system assumptions and stability

A number of conditions on the quantities of Fig. 2 are needed to enable the stability based design of the paper. Regarding the notation of these conditions, $^{(i)}$ denotes differentiation i times and the left half of the complex plane is denoted the LHP. Fig. 1 of [9] clearly contains Fig. 2 of the present paper as a special case. It follows from [9] that the needed conditions are:

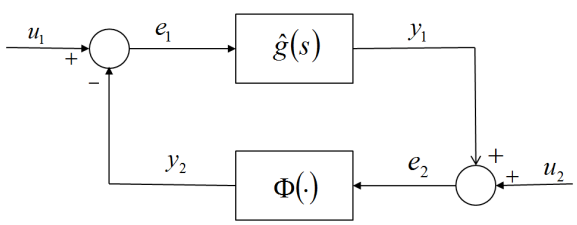

Figure 3: Block diagram for the Popov criterion.

C1) $Re[a_{1,i}] > 0, \quad i = 1, ..., na_1, \quad Re[b_{1,i}] > 0, \quad i = 1, ..., nb_1$, and $G_p > 0$.

C2) $Re[a_{2,i}] > 0, \quad i = 1, ..., na_2, \quad Re[b_{2,i}] > 0, \quad i = 1, ..., nb_2$.

C3) $G_{p,w}(s)$ and $C(s)$ are proper with all poles strictly in the LHP.

C4) $nb_1 \leq na_1$.

C5) $nb_2 \leq na_2$.

C6) At least one of $G_{p,1}(s)$, $G_{p,2}(s)$ and $C(s)$ is strictly proper.

C7) $y_{ref}^{(na_1-nb_1+na_2-nb_2)}(t+T) \in \mathcal{L}_2$.

C8) $w^{(na_1-nb_1)} \in \mathcal{L}_2$, $w^{(na_1-nb_1+1)} \in \mathcal{L}_2$.

C9) $n^{(na_1-nb_1+na_2-nb_2)}(t) \in \mathcal{L}_2$,
$n^{(na_1-nb_1+na_2-nb_2+1)}(t) \in \mathcal{L}_2$.

C10) $\mu_{max} > 0$ and $k_0 > 0$.

C1-C9 form a subset of conditions A1-A16 of [9], while C10 ensures that $0 \leq \sigma\Phi(\sigma) \leq k\sigma^2$. It follows by inspection that the remaining conditions of [9] are automatically fulfilled for the ammonium control system of the present paper. An extensive intuitive explanation of the interpretation of C1-C9 appears in [9] and [10] and is not repeated here. C1-C9 are further discussed in Section 6, and shown to be valid for the treated ammonium control system. To proceed, note that the linear loop gain corresponding to Fig. 2 is

$$\hat{g}(s) = e^{-sT}C(s)G_{p,1}(s)G_{p,2}(s). \tag{12}$$

The conditions C1-C10 and Lemma 2 of [9] now implies

Theorem 1: Consider the ammonium control system of Fig. 2 and assume that the conditions C1)-C10) hold. Then the ammonium control system is $\mathcal{L}_2$-stable if there exist constants q, $\delta > 0$, such that the Popov plot of

$$\hat{g}(s) = e^{-sT}C(s)G_{p,1}(s)G_{p,2}(s),$$

given by

$$\omega \in [0, \infty) \rightarrow Re[\hat{g}(j\omega)] + j\omega Im[\hat{g}(j\omega)] \in C$$

lies entirely to the right of a line through $-1/k + \delta + j0$ with slope $1/q$, for some $q \geq 0$ and some $\delta > 0$.

Proof: See [9], proof of Lemma 2.

5.3. Control system design by stability region pre-computation

To select a controller rendering an $\mathcal{L}_2$-stable system, the stability region represented by $\hat{g}(s)$ is calculated as a function of a set of controller parameters. The parameter set is defined by the controller proportional and integral gains, K_P and K_I respectively, and by the leakage, α. The time delay, T, describes the uncertainty of the system and quantifies the stability region in this work.

Algorithm 1 starts with a definition of the parameters and uncertainty grids and returns the maximum allowed time delay T_{max} for the control system to be within the stability region.

Algorithm 2 Stability region pre-computation

Parameter grid $[P_1...P_i]$, delay grid $[T_1...T_j]$, line grid $[q_1...q_m]$, frequency grid $[\omega_1...\omega_n]$
for $P = P_1, ..., P_i$ **do**
  for $T = T_1, ..., T_j$ **do**
    $found_q = 0$
    for $q = q_1, ..., q_m$ **do**
      for $\omega = \omega_1, ..., \omega_n$ **do**
        $\hat{g}(jw) = e^{-sT}C(jw)G_{p,1}(jw)G_{p,2}(jw)$
        $Re[\hat{g}(j\omega)] + qj\omega Im[\hat{g}(j\omega)]$
      end for
      if $Re[\hat{g}(j\omega)] + qj\omega Im[\hat{g}(j\omega)] > -1/k \ \forall \ \omega$ **then**
        $found_q = 1$
      end if
    end for
    if $found_q = 0$ **then**
      $T_{max}(P) = T$
      $break$
    end if
  end for
end for

For each parameter grid point, the loop is performed over all Popov lines, q, and the Popov inequality is evaluated according to Theorem 1. If the inequality holds for all w, the next value of q is considered. If no such line is found, i.e. if the boolean variable $found_q = 0$, the stability limit, T_{max} is assigned. Note that a similar algorithm was used in [10] and the references therein. The stability based design is hence applicable to other linear asymptotically stable controllers like the H_∞ controller of [10].

Note that the Popov condition is sufficient for $\mathcal{L}_2$-stability. The com-

puted stability region hence predicts stability for K_P, K_I and α that are in the region. However, it does not necessarily predicts instability outside the predicted stability region. The computed region is therefore a subset of the complete stability region.

6. Results

6.1. Identification

For the experiment, data was simulated using the BSM1 environment described in Section 4.2, in an open loop case with the DO set point selected as a time-varying reference signal being the input to the system. To simulate the concentration level, the input signal was created from a pseudorandom binary sequence (PRBS) multiplied by samples from a uniformly independent and identically distributed probability function, c.f. [17]. The input signal is characterised by a mean value of 2 g/m^3 and a maximum amplitude of 1.5 g/m^3 which are consistent with the physical properties of the system.

To match the BSM1 dynamics, where the plant is simulated over days with a sampling period of 1/96 days, the time scale of the transfer function was changed to the corresponding size and units. Hence, the studied plant was simulated over 12 days with a sampling period of 15 minutes.

In [7], the identification was performed using a time-varying influent as disturbance. However, for simplicity, here the simulations were performed for constant influent data with the inflow rate, Q_{in}, set to 20514 m^3/day and the influent ammonium concentration, $NH_{4,in}$, equal to 31.6 g/m^3.

The output signal is the measured concentration level of the ammonium at the outlet of the system. White noise was added to the output signal to model the measurement noise of the sensor.

The Monod Hammerstein modelling method of Section 3 was used for the identification. The polynomial orders were chosen experimentally by performing Monte Carlo simulations over a range of model orders. The result was evaluated using a validation data set and showed that the best percentage fit of 70.4% was obtained for the orders $(n_a, n_b, n_k) = (6, 5, 11)$. Here, n_a represents the denominator order, n_b the numerator order and n_k the delay mainly caused by the settler in terms of the number of samples. The saturation constant k_o of the Monod function was estimated to 0.1, obtained by the method described in Section 3. Fig. 4 shows the obtained identification results for the validation data set.

The model obtained from the $MATLAB^{TM}$ *oe* function, is given by the

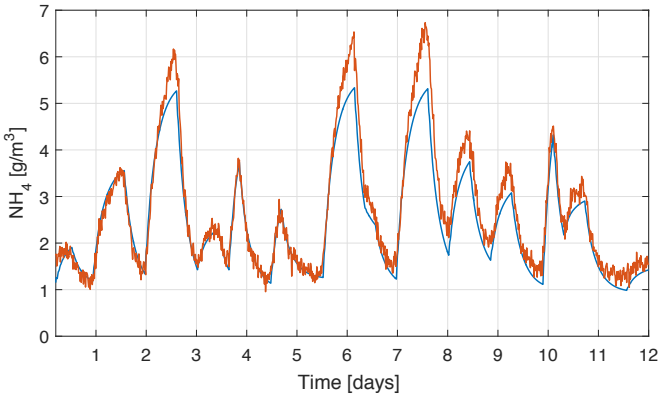

Figure 4: Identification results obtained by the Monod Hammerstein model: red - real data, blue - estimated model.

transfer function operator

$$G^d_{p,1}(q)G^d_{p,2}(q) = G^d_p(q) = \frac{B^d(q)}{A^d(q)}, \tag{13}$$

where

$$B^d(q) = -5.92q^{-11} + 7.41q^{-12} - 2.17q^{-13} - \\ - 0.02q^{-14} - 0.06q^{-15}, \tag{14}$$

$$A^d(q) = 1 - 2.04q^{-1} + 1.6q^{-2} - 1.08q^{-3} + \\ + 0.66q^{-4} - 0.02q^{-5} - 0.1q^{-6}, \tag{15}$$

where q^{-11} corresponds to the output delay q^{-n_k}.

After obtaining the discrete time model, the plant transfer function $G^d_p(q)$ was transformed to a continuous time model in order to allow the controller design procedure outlined above. This was done using the function *d2c* of the $MATLAB^{TM}$ Control System toolbox, [24], which converts a discrete time model to a continuous time one applying ZoH sampling. The transformation to continuous time resulted in

$$e^{-sT}G_p(s) = e^{-sT}\frac{B(s)}{A(s)}, \tag{16}$$

where e^{-sT} is the delay transfer function in continuous time, $T = 0.0104$ days, and

$$B(s) = -380s^6 - (1.95 \cdot 10^5)s^5 - (7.5 \cdot 10^7)s^4 - \\ - (1.39 \cdot 10^{10})s^3 - (1.47 \cdot 10^{12})s^2 - (6.63 \cdot 10^{13})s - 1.06 \cdot 10^{15}, \quad (17)$$

$$A(s) = s^7 + 335.9s^6 + (1.59 \cdot 10^5)s^5 + (1.89 \cdot 10^7)s^4 + \\ + (3.52 \cdot 10^9)s^3 + (1.5 \cdot 10^{11})s^2 + (3.2 \cdot 10^{12})s + 1.16 \cdot 10^{13}. \quad (18)$$

Note that the increase of the order is due to the fact that the discrete time model has a stable pole on the negative real axis, in such cases the $MATLAB^{TM}$ function increases the order one step, see [24]: "When you call *d2c* without specifying a method, the function uses ZoH by default. The ZoH interpolation method increases the model order for systems that have real negative poles. This order increase occurs because the interpolation algorithm maps real negative poles in the z domain to pairs of complex conjugate poles in the s domain."

6.2. Stability region

For the computation of the stability region, the loop gain of the system described in Fig. 2 is studied. This is given by

$$\hat{g}(s) = e^{-sT}C(s)G_p(s), \quad (19)$$

where $G_p(s)$ of (16) – (18) describes the plant dynamics obtained experimentally in Section 4.2. The controller $C(s)$ is selected to be a PI controller with leakage as discussed in Section 4.2.

In order for the stability based design to be relevant, the conditions imposed for Theorem 1 need to be checked. Referring to the continuous time transfer functions of the identified system (16) – (19) and the controller (6) it follows by observation and trivial computations that C1, C2, C3, C4, C5 and C6 hold. C8 can be disregarded since the disturbance $w(s)$ is constant here. The conditions C7 and C9 are dependent on the selection of the reference and the noise, however these conditions are mild and can be expected to hold in practice. In essence, C7 and C9 ensure that the high frequency contents of the signals roll off sufficiently fast. Finally, C10 is met by inspection of the identified Monod function.

To compute projections of the subset of the stability region, the following cases were considered:

1. K_P fixed to -0.2, K_I and α varied.

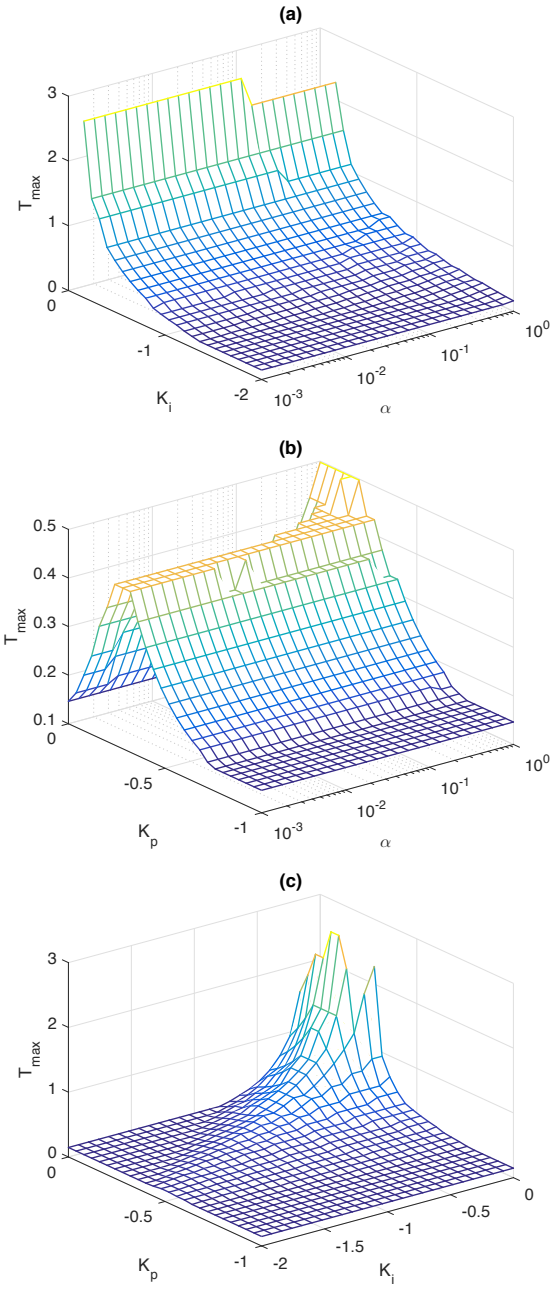

Figure 5: The maximum time delay resulting in $\mathcal{L}_2$-stability according to Eq. 11. (a) K_P is fixed, K_I and α are changing, (b) K_I is fixed, K_P and α are changing, (c) α is fixed, K_P and K_I are changing. T_{max} is given in days.

2. K_I fixed to -0.85, K_P and α are varied.

3. α fixed to 0.001, K_P and K_I are varied.

Fig. 5 shows the surfaces represented by the maximum allowed delay for each of the cases 1-3. Small values of the leakage α give tighter stability regions, see Fig. 5 (b). This is predicted by [10]. A decrease in the proportional gain first gives a larger allowed time delay of the system, Fig. 5 (b). For too low K_P, the integrating part of the controller does, however, become dominating and starts to reduce the stability margin, see Fig. 5 (b) and Fig. 5 (c). A decrease of K_I seems to be uniformly beneficial for stability.

To illustrate the use of Theorem 1, different time delays were tested on the closed loop system using the nominal controller of the cases 1-3. Results are shown in Fig. 6. As can be seen, it is always possible to draw a line through $-1/k + \delta + j0$ so that the Popov plot remains on the right side of the Popov line.

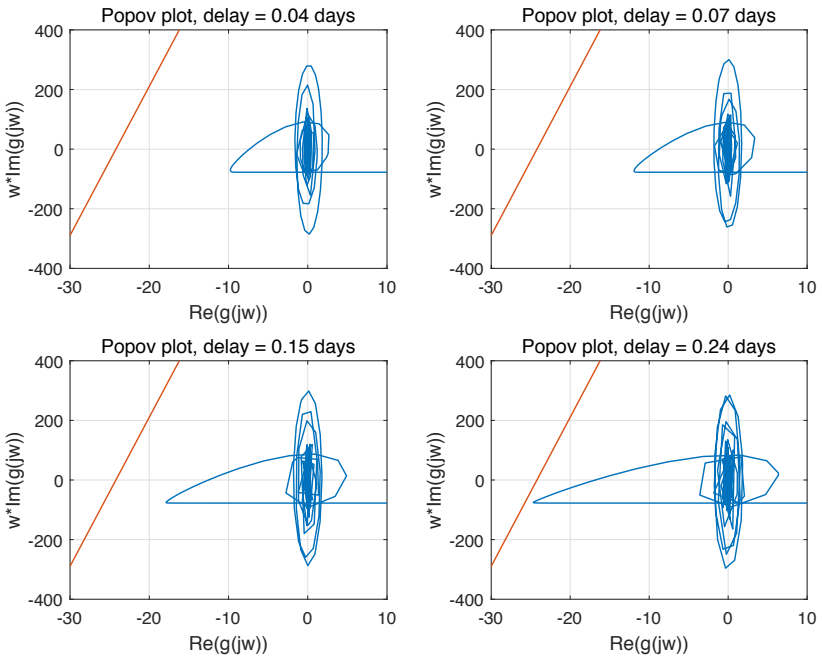

Figure 6: Popov plots for different time delays.

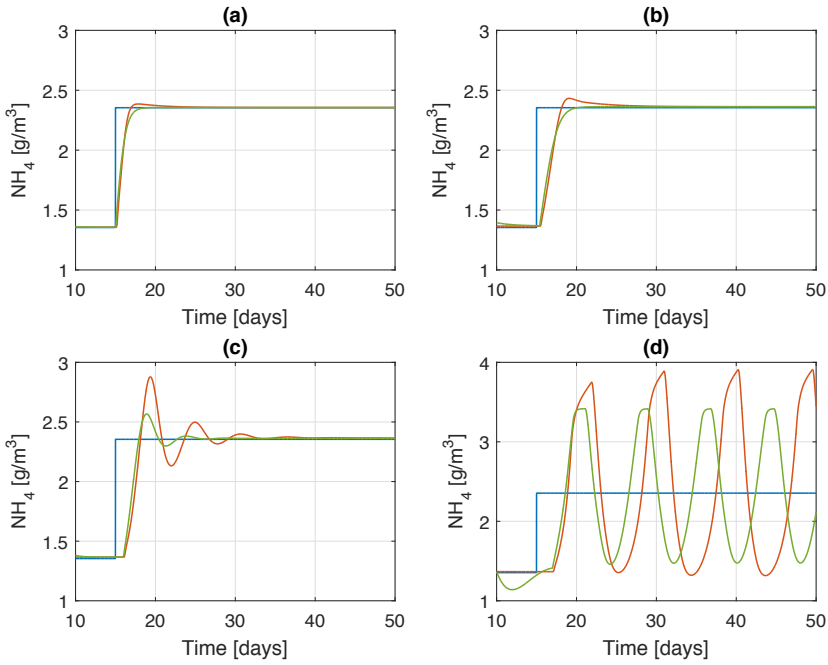

Figure 7: Step response of a nominal controller (a), of a new controller with an additional time delay 0.4 days (b), 1 day (c) and 2 days (d). Blue lines show the reference signal, red lines - the BSM1 output signal, green lines - identified Hammerstein model output.

6.3. Ammonium control performance

As a final part of the numerical study, a retuned controller with settings chosen from the stability analysis computations was tested on the modified BSM1 simulator and the estimated Hammerstein model. In order to evaluate the effect of different time delays, an additional time delay, $\Delta T \geq 0$, was used to delay the output signal of the system. The selected controller parameters were $K_P = -0.1$, $K_I = -0.4$ and $\alpha = 0.0024$, located in the interior of the stability region. The performance was evaluated using a step response of the reference signal. The results are shown in Fig. 7, where different values of the delay ΔT were selected: one within the stability region, Fig. 7(b), one on the border of the stability region, Fig. 7(c), and one outside the stability region, Fig. 7(d). Fig. 7(a) shows the step response of the nominal controller defined in the previous section.

The identified Hammerstein system behaves as expected from the stability region computations, considering the additional delay. The response of

the modified BSM1 model shows a similar behaviour to the nominal controller. Larger delays give a more oscillating response, while the delay exceeding the stability region values leads to an unstable system, as was predicted by the stability analysis. It needs to be noted that the complete system model is less stable than the one based on the Hammerstein model.

The feedback control prevents the control system to enter a very high concentration region where the identified model is less accurate, as can be seen in Fig. 4. Normally, such high concentration set points are avoided in practice. Additional evaluation of this case is yet relevant, e.g. to handle large disturbances. This will be the subject of future research.

7. Conclusion

A new tuning method for an ammonium feedback controller was suggested for an aeration control loop in a nitrifying activated sludge process in a wastewater treatment plant. An identification of a Hammerstein model was performed as a pre-requisite for the controller design. The main objective of the paper was to introduce an approach to obtain a robustly stable closed loop performance of the system in terms of $\mathcal{L}_2$-stability. Therefore, the Popov inequality corresponding to the Hammerstein model was used for the computation of a subset of the stability region, the subset being represented by a maximum allowed delay.

The performance of the controller with parameters chosen from the obtained stability region was tested in a simplified version of the simulation environment BSM1. The simulations show that the identified Hammerstein model appears accurate enough for the robust stability to carry over to the full benchmark simulation model. In practice, additional effects may, however, need to be accounted for, which is why testing of the proposed method in e.g. a pilot plant would be a natural topic for further research. In addition, future research could also be focused on a further use of the identified nonlinearity. Here, gain-scheduling, model predictive control and partial inversion of the nonlinearity are interesting alternatives.

Bibliography

[1] G. Tchobanoglous, F. L. Burton and H.D. Stensel, *Wastewater Engineering: Treatment and Reuse*. Metcalf & Eddy, Inc., New York, NY: McGraw-Hill, 2003.

[2] M. H. Gerardi, *Nitrification and Denitrification in the Activated Sludge Process.* New York, NY, USA: Wiley, 2003.

[3] L. Åmand, C. Laurell, K. Stark-Fujii and B. Carlsson, "Lessons learnt from evaluating full-scale ammonium feedback control in three large wastewater treatment plants", *Water Science and Technology*, vol. 69(7), pp. 1573-1580, 2014.

[4] L. Åmand, G. Olsson and B. Carlsson, "Aeration control - a review", *Water Science and Technology*, vol. 67(11), pp. 2374-2398, 2013.

[5] K. V. Gernaey, M. C. M. van Loosdrecht, M. Henze, M. Lind and S. B. Jørgensen, "Activated sludge wastewater treatment plant modelling and simulation: state of the art ", *Environmental Modelling & Software*, vol. 19, no. 9, pp. 763-783, 2004.

[6] M. Henze, "Activated sludge model no. 1", *IAWPRC Scientific and Technical Reports*, 1, London, UK: IWA Publishing, 1987.

[7] T. Chistiakova, B. Carlsson and T. Wigren, "Non-linear modeling of the dissolved oxygen to ammonium dynamics in a nitrifying activated sludge process", *Proc. ICA 2017*, Quebec City, Quebec, Canada, pp. 85-93, June 11-14, 2017.

[8] L. Åmand, "Ammonium feedback control in wastewater treatment plants", Ph.D. thesis, Uppsala University, Uppsala, Sweden, 2014. Available on-line at http://uu.diva-portal.org.

[9] T. Wigren, "Low-frequency limitations in saturated and delayed networked control", *Proc. IEEE CCA 2015*, Manly, Sydney, NSW, Australia, pp. 564-571, 2015.

[10] T. Wigren, "Low frequency sensitivity function constraints for nonlinear $\mathcal{L}_2$-stable networked control", *Asian J. Contr.*, vol. 18, no. 4, pp. 1200-1218, 2016.

[11] G. Olsson and B. Newell, *Wastewater Treatment Systems: Modeling, Diagnosis and Control*, London, UK: IWA Publishing, 1999.

[12] G. Olsson, M. Nielsen, Z. Yuan, A. Lynggaard-Jensen and J. Steyer, *Instrumentation, Control and Automation in Wastewater Systems*, London, UK: IWA Publishing, 2005.

[13] J. B. Copp (ed.), *The COST Simulation Benchmark - Description and Simulator Manual*, Office for Official Publications of the European Communities, ISBN 92-894-1658-0, Luxembourg, 2002.

[14] L. Ljung, *System Identification: Theory for the User.* Upper Saddle River, NJ, USA: Prentice Hall, 1999.

[15] L. Ljung, *System Identification Toolbox: Users Guide Version 7.4.* Natick, MA, USA: The Mathworks, 2011.

[16] P. Mattsson and T. Wigren, "Convergence analysis for recursive Hammerstein identification", *Automatica*, vol. 71(C), pp. 179-186, 2016.

[17] T. Chistiakova, P. Mattsson, B. Carlsson and T. Wigren, "Nonlinear system identification of the dissolved oxygen to effluent ammonia dynamics in an activated sludge process", *Proc. IFAC 2017 World Congress*, Tolouse, France, pp. 3978-3983, July 9-15, 2017.

[18] G. C. Goodwin, M. M. Seron and J. A. DeDona, *Constrained Control and Estimation - An Optimization Approach.* London, UK: Springer-Verlag, 2005.

[19] M. Ekman, "Bilinear black-box identification and MPC of the activated sludge process", *J. Process Contr.*, vol. 18, no. 7, pp. 643-653, 2008.

[20] J. Monod, "The growth of bacterial cultures", *Annual Review of Microbiology*, vol. 3, pp. 371-394, 1949.

[21] T. Söderström and P. Stoica, *System identification.* Hemel Hempstead, UK: Prentice-Hall, 1989.

[22] T. Glad and L. Ljung, *Control Theory.* Bodmin, UK: Taylor and Francis, 2000.

[23] M. Vidyasagar, *Nonlinear Systems Analysis.* Englewood Cliffs, NJ, USA: Prentice-Hall, 1978.

[24] MathWorks, Inc, *Control system toolbox for use with $MATLAB^{TM}$: getting started.* Natick, MA, USA: The Mathworks, 2005.

Paper IV

Combined $\mathcal{L}_2$-stable Feedback and Feedforward Aeration Control in a Wastewater Treatment Plant

Tatiana Chistiakova, Torbjörn Wigren and Bengt Carlsson [1]

Abstract

A nitrifying activated sludge process with ammonium feedback and disturbance feedforward control is studied. The feedback and feedforward measurements are subject to time delay and the control loop includes a saturation. A Hammerstein based model is identified, including process delays and the nonlinearity. The proposed feedback control strategy includes tuning of a linear lag compensator that has a limited low-frequency gain which allows global stability to be established with the Popov criterion. The feedforward controller attenuates the disturbance and provides an overall improvement of the control strategy. The performance of the combined feedback and feedforward aeration controller is evaluated with a benchmark model.

[1]Department of Information Technology, Uppsala University, SE 75105 Uppsala, Sweden

1. Introduction

A wastewater treatment plant (WWTP) has a large-scale, nonlinear and complex structure. Controlling and monitoring its processes are demanding and complicated tasks. The variety in plant configurations makes it intricate to implement and to evaluate control strategies to get results of general validity. When studying WWTPs, two aspects are of a major interest: efficiency and low operational cost, [1]. One of the most energy consuming processes in a WWTP is the aeration of water when biological nitrogen is removed in an activated sludge process (ASP), [2]. Oxygen supply is crucial for microorganisms to grow in the aerobic part, so the concentration level of dissolved oxygen (DO) should be high enough but not exceeding a certain level to avoid sludge deterioration, [3]. Moreover, a high air flow rate may result in an excessive energy consumption.

The reasoning behind DO level control is therefore twofold, reflecting both economical and process demands. A common approach is to set a predefined DO concentration in the water, [4]. However, this approach has shown some disadvantages, like increased energy consumption. As an alternative, aeration control using feedback from ammonium measurements has shown to be a useful tool for minimising energy costs but still maintaining the effluent water quality, [5], [6] and [7]. Also, various implementation of feedforward control have shown promising results. For example, [8] presents feedforward control using ammonium measurements taken prior to the aeration line. The experiment indicated a sufficient DO concentration control performance resulting in a decreased energy consumption. The presence of influent ammonium peaks allows another possible use of feedforward control within the ASP. This aspect is described in [9] and [10], where advantages and disadvantages of the feedforward control strategy are presented in a structured way and compared with a common feedback aeration control. However, these studies are limited to an implementation in a specific plant. Additionally, the time delays are not accounted in the controller design.

The present paper is motivated by the potential gains that are expected to follow from an efficient automation of the ammonium control process. A specific aspect of the paper is that it accounts for the delays between the DO and effluent amonium concentration and between the wastewater inflow and the ammonium concentration.

The DO to ammonium dynamics is highly nonlinear due to various factors, like the growth rate of bacteria, and the concentration saturation of DO and air valves. These factors impose additional challenges on the control process. Therefore, nonlinear system identification is used to obtain a more simple model. This is the first contribution of the paper. The model is chosen to have a Hammerstein structure, with a static nonlinear

input function described by a Monod function. It allows incorporation of the saturation associated with the aeration controllers in the wastewater. The nonlinear biological and fluid dynamics of three aerobic bioreactors are thus approximated by the combined effect of the static nonlinearity and linear dynamics of the identified Hammerstein model. Also, the system is assumed to be affected by the disturbance signal, constituted by the varying inflow of wastewater. The Hammerstein grey-box identification algorithm, extended from [11] and [12], is used to derive the model of the system and the disturbance from high fidelity simulated data.

The second contribution consists of a study of the feedback control loop together with the delay associated with the measurement of the ammonium concentration at the outlet of the bioreactors. The presence of a saturation and a large delay in the control loop led to a controller design method accounting for the low frequency gain of the loop, as in [13] and [14]. As in [15], a pre-computation of a projection of a subset of the $\mathcal{L}_2$ stability region is performed, based on the Popov inequality. In addition, feedforward, [16], [17], from the wastewater inflow is added to further suppress the disturbance.

The third contribution evaluates this combination of a tuned feedback controller with feedforward. The evaluation is performed using a benchmark simulation environment.

The paper is organised as follows. The investigated system is described in Section 2. The identification and controller design is presented in Sections 3 and 4, respectively. Section 5 analyses the stability conditions of the system. Finally, the numerical experiment is given in Section 6 followed by conclusions in Section 7.

2. System description

2.1. Wastewater treatment plant aspects

A wastewater treatment process is composed of several steps: physical, biological and chemical treatment. During biological treatment, one of the commonly applied methods is an Activated Sludge Process (ASP), where various microorganisms are involved. In particular, aerobic bacteria are used in aeration bioreactors for an ammonium oxidation. Therefore, a sufficient supply of oxygen is required in every aerobic bioreactor.

2.2. Simulation model

A very popular mathematical model of the biological process in an ASP is the Activated Sludge Model no.1 (ASM1), [18]. The model represents core biological processes (organic matter removal, nitrification and deni-

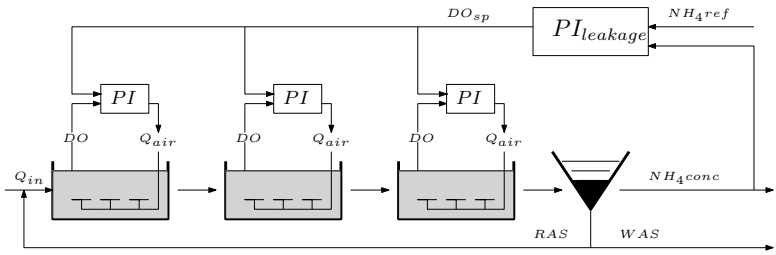

Figure 1: Schematic representation and control structure of an ASP. Q_{in}-inflow, DO_{sp}-DO set point, PI-oxygen supply proportional integral controller, $PI_{leakage}$-DO_{sp} proportional integral controller with leakage, Q_{air}-airflow rate, NH_4conc-ammonium concentration level, NH_4ref - ammonium reference value, RAS-return activated sludge, WAS-waste activated sludge.

trification) with 13 process variables, 19 model parameters and 8 process equations. Therefore, the ASM1 is known for its nonlinear and high order characteristics.

Based on the ASM1, a simulation environment of an ASP was developed for evaluation and comparison of various control strategies. This model is named the Benchmark Simulation Model no.1, [19], and it has been used as a simulating, testing and verification tool. The model implements a typical ASP layout with two anoxic and three aerobic biological compartments, which are designed according to the ASM1, and a settler. Different input data files are available to simulate various weather conditions. In this work, a reduced version of BSM1 is used where only aerobic bioreactors are considered.

Fig. 1 gives a schematic representation of an ASP process with an ammonium control structure. Here, the set point for the DO controllers is provided by an ammonium controller. As mentioned before, the relation between the signals is nonlinear. Also, the DO set point is subject to saturation. The time delay occurs after the settler where the ammonium measurements are done, and causes an additional challenge when studying control and stability.

3. Hammerstein identification

To enable controller design, the system is identified using a nonlinear identification method. However, identification with the standard black-box methods of the $MATLAB^{TM}$ System Identification Toolbox, [23] may give a

complicated model resulting in a complicated controller. One reason is that the static nonlinearity is modelled as piecewise linear, which requires a significant number of parameters. As a an alternative, a nonlinearity described by a static Monod function, [20], is used here. This allows identification of a model with fewer parameters than the standard choice of black-box model. This nonlinearity can be represented as

$$\hat{u}(t) = \mu_{max} \frac{\bar{u}(t)}{\bar{u}(t) + k_o}, \tag{1}$$

where $\bar{u}(t)$ is the DO set point, μ_{max} is the maximum growth rate set to the constant value 0.5 and k_o is the half saturation constant, [19], that is chosen experimentally by gridded optimisation over a set of values in the present paper.

The Hammerstein model therefore has the following structure

$$\hat{y}(t) = \frac{B_{d,p}(q)}{A_{d,p}(q)} \hat{u}(t) + \frac{B_{d,w}(q)}{A_{d,w}(q)} w(t), \tag{2}$$

where $\hat{u}(t)$ is the input signal and $w(t)$ is the disturbance signal. $B_{d,p}(q)$, $A_{d,p}(q)$, $B_{d,w}(q)$ and $A_{d,w}(q)$ are polynomials for the input and disturbance signals, respectively, [21], given in discrete time as indicated by the subscript d

$$B_{d,i}(q) = b_{1,i} q^{-n_{k,i}} + ... + b_{n_{b,i}} q^{-n_{k,i} - n_{b,i} + 1}, \tag{3}$$

$$A_{d,i}(q) = 1 + a_{1,i} q^{-1} + ... + a_{n_{a,i}} q^{-n_{a,i}} \tag{4}$$

with q^{-1} being the backward shift operator, $n_{b,i}$ and $n_{a,i}$ are the polynomials orders, $n_{k,i}$ is the input delay defined as the number of samples. The function $\hat{u}(t)$ is a static nonlinearity described by (1). In (3) and (4), the subscript i takes the values p for the plant and w for the disturbance.

In order to identify the linear part of (2), the $MATLAB^{TM}$ function *oe* is applied. The function is a common tool in linear system identification and it is implemented using the output error algorithm, see [23] for more details.

4. Controller design

The fundamental stability based design is formulated in continuous time. Since the identified model is obtained in discrete time, it is converted to continuous time prior to the controller design, [22].

The ammonium control system is shown in Fig. 2. Here, $y_{ref}(s)$ is the ammonium reference set point, $C_{fb}(s)$ is the DO feedback controller filter,

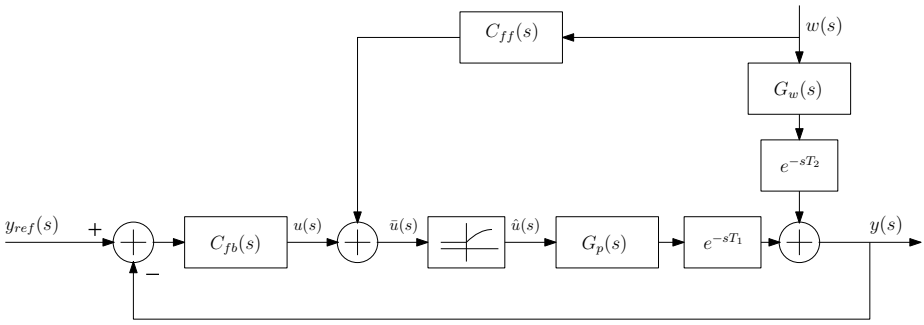

Figure 2: Complete block diagram of the control system.

$G_p(s)$ is the plant transfer function, $G_w(s)$ is the disturbance transfer function, $C_{ff}(s)$ is the feedforward controller filter and $y(s)$ is the ammonium concentration measured after the settler. The time delays, e^{-sT_1} and e^{-sT_2}, are also obtained from the identified model. s is the independent variable of the Laplace transform.

4.1. Feedback controller with leakage

The proportional integral (PI) controller is widely used in the wastewater treatment community and is well known by many plant operators. It is a simple but efficient technique that with some modification allows the Popov criterion to be applied for stability analysis. For this purpose, a leakage term is added to the integral part aiming to limit the sensitivity function from below, [14], and the low frequency gain from above, [13]. Hence, the feedback controller, $C_{fb}(s)$, is implemented as

$$u(s) = C_{fb}(s)e(s) = \left(K_P + K_I \frac{1}{s+\alpha}\right) e(s), \tag{5}$$

where K_P is the proportional gain, K_I is the integral gain, $\alpha > 0$ is the leakage variable, and the control error $e(s)$ is defined as

$$e(s) = y_{ref}(s) - y(s), \tag{6}$$

where $y_{ref}(s)$ is the set point and $y(s)$ is the controlled signal.

4.2. Feedforward controller

To improve the performance of the control system, the effect of a disturbance on a system may be attenuated by feedforward control, [16]. The perfect theoretical disturbance rejection is obtained by setting the feedforward part

of the control variable so that it eliminates the influence of the disturbance on the system completely.

The transfer function of such a controller is easily obtained from Fig. 2, neglecting the nonlinearity, and it is given by

$$C_{ff}(s) = -e^{-s(T_2-T_1)} K_m \frac{G_w(s)}{G_p(s)}. \tag{7}$$

Here, $G_w(s)$ is the disturbance transfer function and $G_p(s)$ is the plant transfer function of the block diagram of Fig. 2, K_m is the gain of the nonlinearty approximating the effect of the Monod function at the selceted operating point.

However, in this application $T_2 < T_1$. In such a case (7) is infeasible and can not be implemented. Therefore, (7) is here approximated with

$$C_{ff}(s) = -K_m \frac{G_w(s)}{G_p(s)}. \tag{8}$$

Note that (8) also requires that $G_w(s)$ is asymptotically stable and that $G_p(s)$ is (strictly) minimum phase. The rationale behind the choice (8) is that, as shown by the identification experiments of Section 6.2, the difference between T_1 and T_2 is small. Therefore, the phase of (8) can be expected to be quite close to the phase of (7) for reasonably high bandwidths. In cases where the signals remain close to the operating point represented by K_m and the bandwidth is not too high, a good suppression of the disturbance could therefore be expected. There are many more advanced ways to design feedforward controllers, see e.g. [16]. However, due to the nonlinear effects such optimal linear feedforward designs may anyway not provide significant gains over the present choice. This provides a motivation for the more simple approach represented by (8). More research is however needed on this subject.

5. Stability analysis

5.1. Popov criterion

Since the control system contains the infinite dimensional transforms e^{-sT_1} and e^{-sT_2}, input-output stability as defined in [24] is applied for the stability analysis of the system of Fig. 2. For completeness, the definitions underpinning the analysis are

Definition 1: For all $p \in [1, \infty)$, $\mathcal{L}_p[0, \infty)$ denotes the set of func-

tions $f(\cdot) : [0, \infty) \to \mathcal{R}$, such that

$$\|f(\cdot)\|_p^p = \int_0^\infty |f(t)|^p dt < \infty.$$

Definition 2: The set of functions $f(\cdot) : [0, \infty) \to \mathcal{R}$, so that their truncations

$$f_T(t) = \begin{cases} f(t), & 0 \le t \le T \\ 0, & t > T \end{cases} \in \mathcal{L}_p[0, \infty),$$

$\forall T$, is the extension $\mathcal{L}_{pe}[0, \infty)$ of $\mathcal{L}_p[0, \infty)$.

Definition 3: The mapping $A : \mathcal{L}_{pe} \to \mathcal{L}_{pe}$ is $\mathcal{L}_p$-stable if $Af \in \mathcal{L}_p$ whenever $f \in \mathcal{L}_p$, and finite constants l, c exist, so that

$$\|Af\|_p \le l\|f\|_p + c, \quad \forall f \in \mathcal{L}_p.$$

Definition 4: $\mathcal{A}$ is the set of generalized functions

$$f(t) = \begin{cases} 0, & t < 0 \\ \sum_{i=0}^\infty f_i \delta(t - t_i) + f_a(t), & t \ge 0 \end{cases}$$

where $\delta(\cdot)$ is the unit delta distribution, t_i are non-negative constant delays, $f_a(t)$ is measurable and

$$\sum_{i=0}^\infty |f_i| < \infty, \qquad \int_0^\infty |f_a(t)| dt < \infty.$$

Definition 5: $\hat{\mathcal{A}}$ is the set of all function $\hat{f} : \mathcal{C}_+ \to \mathcal{C}$ that are Laplace transforms of elements of $\mathcal{A}$.

The analysis applies the Popov criterion which is valid for Fig. 3 and given by

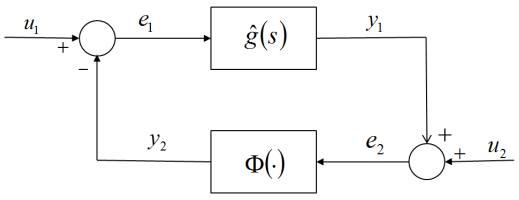

Figure 3: Block diagram for the Popov criterion.

Lemma 1 (Popov Criterion, [24] Theorem 6.7.63): Assume that the inverse Laplace transform of the transfer function $\hat{g}(s)$ fulfils

$$g(\cdot) \in \mathcal{A}, \quad \dot{g}(\cdot) \in \mathcal{A},$$

that the time invariant static nonlinearity $\Phi(\cdot)$ fulfils

$$0 \leq \sigma\Phi(\sigma) \leq k\sigma^2,$$

and that $u_1 \in \mathcal{L}_2$, $u_2 \in \mathcal{L}_2$, $\dot{u}_2 \in \mathcal{L}_2$.

Under these conditions the system is $\mathcal{L}_2$-stable if there exist constants q, δ, such that the Popov plot

$$\omega \in [0, \infty) \rightarrow Re[\hat{g}(j\omega)] + j\omega Im[\hat{g}(j\omega)] \in C$$

lies entirely to the right of a line through $-1/k + \delta + j0$ with slope $1/q$, for some $q \geq 0$ and some $\delta > 0$.

5.2. Signal re-definition

The next step is to prove that the Popov criterion of *Lemma 1* is valid for the control system of Fig. 2. To do so, the quantities $\hat{g}(s)$, u_1 and u_2 of Fig. 3 need to be computed in terms of the corresponding quantities of Fig. 2. Note that the signal $e_2(s)$ of Fig. 3 is the signal $\bar{u}(s)$ of Fig. 2 entering the static nonlinearity and $y_2(s)$ is the one at the output of the nonlinearity shown as $\hat{u}(s)$ in Fig. 2 . It then follows that

$$\begin{aligned} \bar{u}(s) = u(s) + G_{ff}(s)w(s) = C_{fb}(s)y_{ref}(s) \\ + \left(C_{ff}(s) - C_{fb}(s)e^{-sT_2}G_w(s)\right)w(s) \\ -C_{fb}(s)e^{-sT_1}G_p(s)\hat{u}(s). \end{aligned} \tag{9}$$

The corresponding computation for Fig. 3 gives

$$e_2(s) = u_2(s) + \hat{g}(s)u_1(s) - \hat{g}(s)y_2(s). \tag{10}$$

An identification of terms between (9) and (10) results in

$$\hat{g}(s) = e^{-sT_1}C_{fb}(s)G_p(s), \tag{11}$$

$$u_1(s) = \frac{C_{fb}(s)}{\hat{g}(s)}y_{ref}(s) = G_p^{-1}(s)e^{sT_1}y_{ref}(s), \tag{12}$$

$$u_2(s) = \left(C_{ff}(s) - C_{fb}(s) G_w(s) e^{-sT_2} \right) w(s). \tag{13}$$

To handle the non-casuality of $u_1(s)$, it is assumed in the analysis that $y_{ref}(s) = e^{-sT_1} \bar{y}_{ref}(s)$, which leads to

$$u_1(s) = G_p^{-1}(s) \bar{y}_{ref}(s). \tag{14}$$

This means that the re-defined reference signal is subject to a delay of T_1.

5.3. Conditions on the control system

To state conditions, the transfer functions of Fig. 2 are parametrised as follows

$$G_p(s) = K_p \frac{(s + z_{p,1}) ... (s + z_{p,nz_p})}{(s + p_{p,1}) ... (s + p_{p,np_p})}, \tag{15}$$

$$G_w(s) = K_w \frac{(s + z_{w,1}) ... (s + z_{w,nz_w})}{(s + p_{w,1}) ... (s + p_{w,np_w})}, \tag{16}$$

$$C_{fb}(s) = K_{fb} \frac{(s + z_{fb,1}) ... (s + z_{fb,nz_{fb}})}{(s + p_{fb,1}) ... (s + p_{fb,np_{fb}})}, \tag{17}$$

$$C_{ff}(s) = K_{ff} \frac{(s + z_{ff,1}) ... (s + z_{ff,nz_{ff}})}{(s + p_{ff,1}) ... (s + p_{ff,np_{ff}})}, \tag{18}$$

where K_p, K_w, K_{fb} and K_{ff} are gains of the plant, the disturbance, the feedback and feedforward controllers, respectively. $z_{p,i}$, $z_{w,i}$, $z_{fb,i}$, $z_{ff,i}$ and $p_{p,i}$, $p_{w,i}$, $p_{fb,i}$, $p_{ff,i}$ represent the respective zeros and poles of the transfer functions. Note that poles and zeros that are complex appear in complex conjugate pairs.

The nonlinearity $\hat{u}(t)$ is given by

$$\hat{u}(t) = \begin{cases} \hat{u}_{max}, & \bar{u}(t) \geq u_{max} \\ \mu_{max} \frac{\bar{u}(t)}{\bar{u}(t) + k_o}, & u_{min} < \bar{u}(t) < u_{max} \\ \hat{u}_{min}, & \bar{u}(t) \leq u_{min}. \end{cases} \tag{19}$$

Next, it follows from *Lemma 1* that since $\dot{\hat{g}}(\cdot) \in \mathcal{A}$ is required, $\dot{\hat{g}}(\cdot)$ needs to be restricted to be asymptotically stable and strictly proper. $\dot{u_2}$ needs to be generated in the same way, while it is sufficient that u_1 is generated by asymptotically stable and proper filtering.

The following conditions are therefore introduced on the control system of Fig. 2, using $(\cdot)^{(k)}$ to denote differentiation k times

C1) $Re[p_{p,i}] > 0, \quad i = 1, ..., np_p, \quad Re[z_{p,i}] > 0, \quad i = 1, ..., nz_p, \quad nz_p \leq np_p.$

C2) $Re[p_{w,i}] > 0, \quad i = 1, ..., np_w, \quad nz_w \leq np_w.$

C3) $Re[p_{fb,i}] > 0, \quad i = 1, ..., np_{fb}, \quad nz_{fb} \leq \ np_{fb}.$

C4) $Re[p_{ff,i}] > 0, \quad i = 1, ..., np_{ff}, \quad nz_{ff} \leq \ np_{ff}.$

C5) $K_p K_{fb} > 0.$

C6) $nz_p + nz_{fb} < np_p + np_{fb}.$

C7) $\bar{y}_{ref}^{(np_{fb}-nz_{fb})}(t) \in \mathcal{L}_2.$

C8) $w(t) \in \mathcal{L}_2$, and $\dot{w}(t) \in \mathcal{L}_2.$

C9) $\mu_{max} > 0$, $k_o > 0.$

5.4. Popov criterion for the ammonium control system

The validity of the Popov criterion can now be verified. Conditions C1), C3), C5), C6) and (11) imply that $\hat{g}(s)$ is strictly proper and asymptotically stable with correct sign, hence $\hat{g}(\cdot) \in \mathcal{A}$ and $\dot{\hat{g}}(\cdot) \in \mathcal{A}$. In the same way, C1) and C7) imply that $u_1 \in \mathcal{L}_2$, while C2) and C8) imply that $\dot{u}_2 \in \mathcal{L}_2$. C9) implies that the static nonlinearity has finite gain which shows that $k > 0$ exists. This proves:

Theorem 1. *Consider the control system of Fig. 2 and assume that conditions C1) - C9) hold. Then, the control system is $\mathcal{L}_2$-stable if there exist constants q, δ such that the Popov plot of*

$$\hat{g}(s) = e^{-sT_1} C_{fb}(s) G_p(s),$$

given by

$$\omega \in [0, \infty) \rightarrow Re[\hat{g}(j\omega)] + j\omega Im[\hat{g}(j\omega)] \in C,$$

lies entirely to the right of a line through $-1/k + \delta + j0$ with slope $1/q$, for $q \geq 0$ and $\delta > 0$.

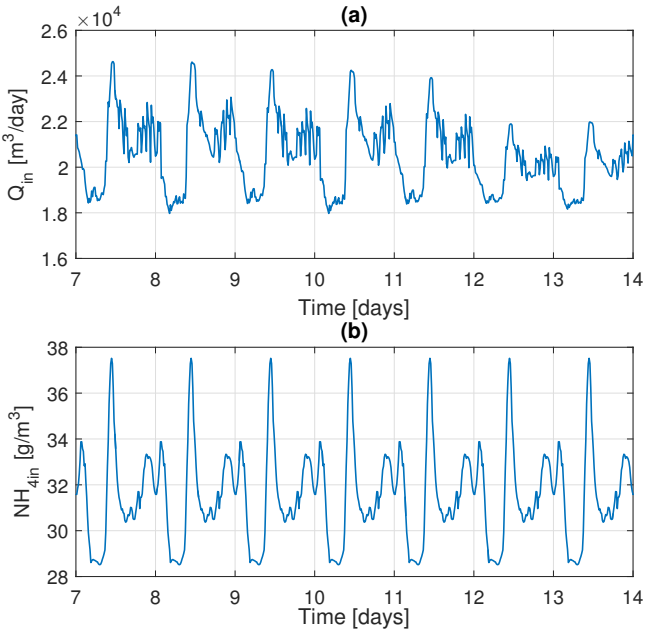

Figure 4: Influent data for dry weather conditions: (a) Inflow rate, Q_{in}, (b) Influent ammonium concentration, NH_{4in}.

6. Results

6.1. Data

The data used for the identification was obtained from the BSM1 environment with three aerobic bioreactors, described in Section 2. The simulation experiment was conducted under dry weather conditions. The simulation time was 7 days with a sampling interval of 15 minutes. Fig. 4 shows an influent flow, $Q_{in}(t)$, and the influent ammonium concentration, $NH_{4in}(t)$, for the dry weather settings.

The BSM1model was simulated as an open loop system, where the DO set point was the input signal, $u(t)$. The input signal was saturated at 0.5 g/m^3 and 3 g/m^3 with a mean value of 1.75 g/m^3 The output, $y(t)$, was the concentration of ammonium after the settler. White noise was added to the output signal replicate a sensor error. An example of the generated data is shown in Fig. 5.

The disturbance signal, $w(t)$, was created based on the inflow rate and

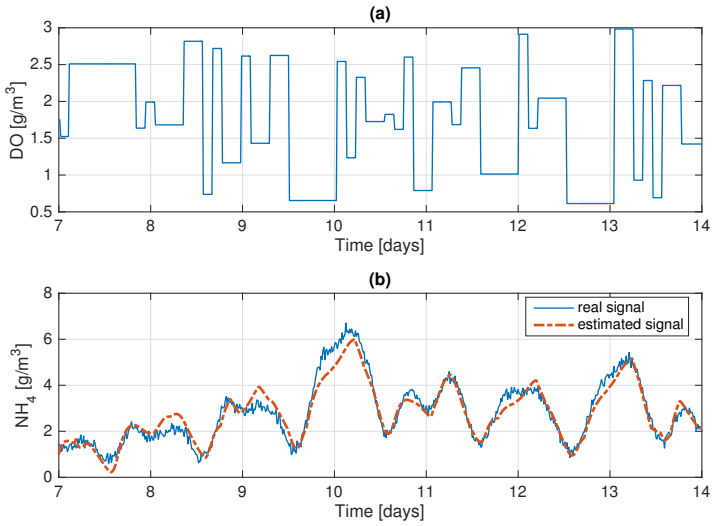

Figure 5: Example of simulated data: (a) Input signal, DO, (b) Output signal, NH_4.

influent ammonium concentration values as follows

$$w(t) = \sigma Q_{in}(t) NH_{4in}(t), \tag{20}$$

where $Q_{in}(t)$ is the inflow rate, $NH_{4in}(t)$ is the influent ammonium concentration and σ is a scaling parameter equal to 10^{-6}.

6.2. Identification

The Hammerstein based identification method with a Monod nonlinearity described in Section 3 was used. The parameter k_o of the nonlinearity (1) was optimised with gridding, resulting in the value $k_o = 0.7$.

The orders of the linear transfer function describing the DO concentration and the disturbance were chosen experimentally and evaluated using a validation data set. The model orders obtained were $(n_{b,p}, n_{a,p}, n_{k,p}) = (1, 1, 19)$ for the DO input and $(n_{b,w}, n_{a,w}, n_{k,w}) = (2, 1, 17)$ for the disturbance signal, where $n_{b,i}$ and $n_{a,i}$ are numerator and denominator order, respectively, and $n_{k,i}$ represent the time delays. The identified model provided a fit of 71.5 % to the validation data, which was evaluated in percent as

$$fit = 100 \cdot \left(1 - \frac{||\mathbf{y} - \hat{\mathbf{y}}||}{||\mathbf{y} - \bar{\mathbf{y}}||}\right).$$

Here, $\mathbf{y}$ is the validation output data, $\hat{\mathbf{y}}$ is the estimated output, $\bar{\mathbf{y}}$ is the mean value of the validation output data and $||\cdot||$ represents a square norm. The identification results are shown with a dashed line in Fig. 5 (b) alongside the validation data.

The structure of the obtained model in continuos time is then

$$y(s) = e^{-sT_1}G_p(s)\hat{u}(s) + e^{-sT_2}G_w(s)w(s), \tag{21}$$

where $T_1 = 0.188$ days and $T_2 = 0.167$ days. The obtained transfer functions are

$$G_p(s) = -98.71\frac{1}{s+2.9},$$

$$G_w(s) = 10.15\frac{s+199.9}{(s+19.9)(s+3.1)}.$$

6.3. Stability region pre-computation

To tune the feedback controller, the method described in [15] was used.

For the pre-computations, a nominal controller was chosen and the following three cases were pre-computed:

1. $K_P = -0.3$, $-2 < K_I < 0$ and $0.001 < \alpha < 1$

2. $K_I = -0.8$, $-1 < K_P < -0.01$ and $0.001 < \alpha < 1$

3. $\alpha = 0.001$, $-1 < K_P < -0.01$ and $-2 < K_I < 0$

The obtained results show the subset of the stability region predicted by the Popov criterion in terms of maximum allowed time delay of the system. The results for every case are shown in Fig. 6.

As follows from Fig. 6 (a), an increased leakage, α, increases the maximum time delay, T_{max}. As shown by Fig. 6 (b), for a fixed K_I, the stability limit increases with K_P up to a certain value, after which it decreases. The reason is that for low K_P, K_I dominates and introduces destabilising phase lag. However, when K_P becomes too large, the high total gain tends to reduce the stability margin. Fig. 6 (c) illustrates the general conclusion that when the control effect is reduced the system becomes more robust to the delay.

6.4. Controller tuning

From the experiment described above, the feedback controller parameters (5) were chosen within the stability region and set to $K_P = -0.7$, $K_I = -0.9$ and $\alpha = 0.005$.

Then, a perfect feedforward controller was chosen, (8), with the following transfer function

$$C_{ff}(s) = -0.058\frac{10.15s + 2029}{98.71(s + 19.9)}.$$

The gain of the nonlinearity, $K_m = 0.058$, was chosen as an approximation of Monod function, (1), around the stable DO set point.

With the obtained model and selected controllers parameters, it is trivial to check that the conditions C1) - C9) hold.

6.5. Control performance

The control system was tested in the simplified BSM1 simulation environment using time-varying conditions together with the disturbance signal. The evaluation was implemented as a comparison of the system performance with feedback only and a combined feedback and feedforward controller.

The results, Fig. 7, show a clear impact of the feedforward controller. With only the feedback controller implemented, the disturbance has a great impact on the ammonium concentration resulting in a big deviation from the reference value, Fig. 7 (b). When the feedforward controller is also introduced, the error decreases significantly allowing the DO set point to adjust for the disturbance effect.

7. Conclusions

The objective of the paper was to design a combined feedback and feedforward ammonium controller, with $\mathcal{L}_2$ - stability guarantees. Prior to control, identification was performed using a Hammerstein model based method with a nonlinearity parameterised as a Monod function. The feedback controller tuning was carried out using the identified model and applying the Popov inequality which allowed pre-compution of the stability region in terms of the maximum allowed feedback loop delay.

Combined with a feedforward controller, the closed loop system was implemented and evaluated in a simplified BSM1 environment. The obtained results show that the proposed controller provides accurate control with robust stability properties, and the feedforward controller improved the performance significantly. A topic for future research may be focused

on a more detailed study of time delay impacts. Possible extensions of the work may also include a test in a complete simulation model followed by test implementation in a pilot plant. A more advanced use of the identified nonlinearity is also planned, applying model predictive control.

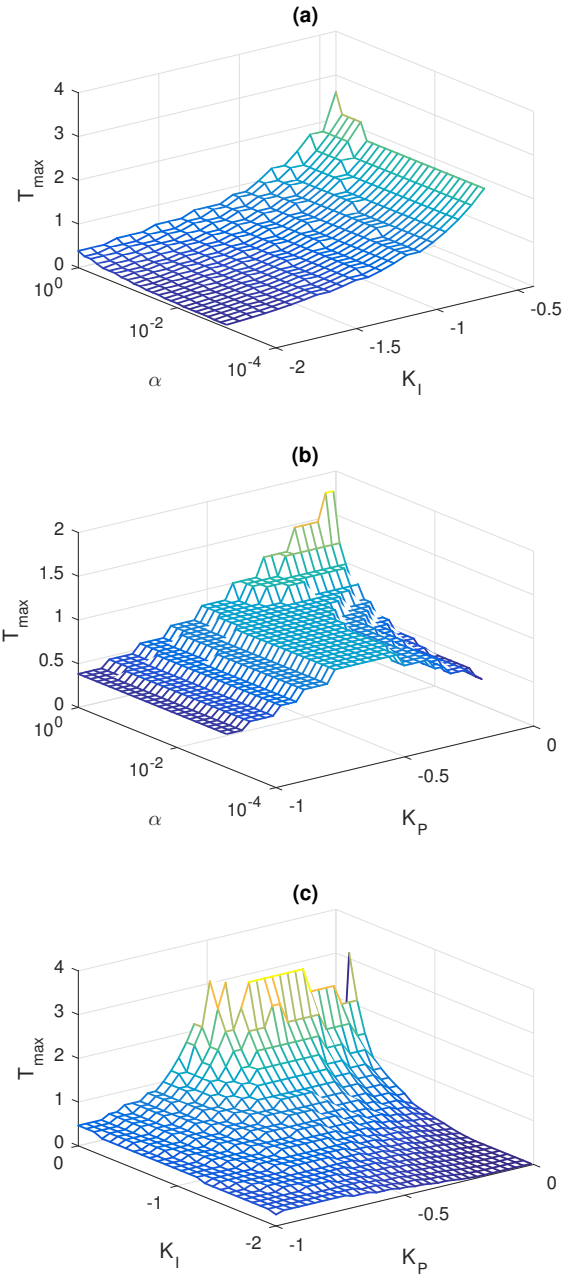

Figure 6: Stability regions expressed by the maximum allowed time delay computed for three cases: (a) K_P fixed, K_I and α vary, (b) K_I fixed, K_P and α vary, (c) α fixed, K_P and K_I vary.

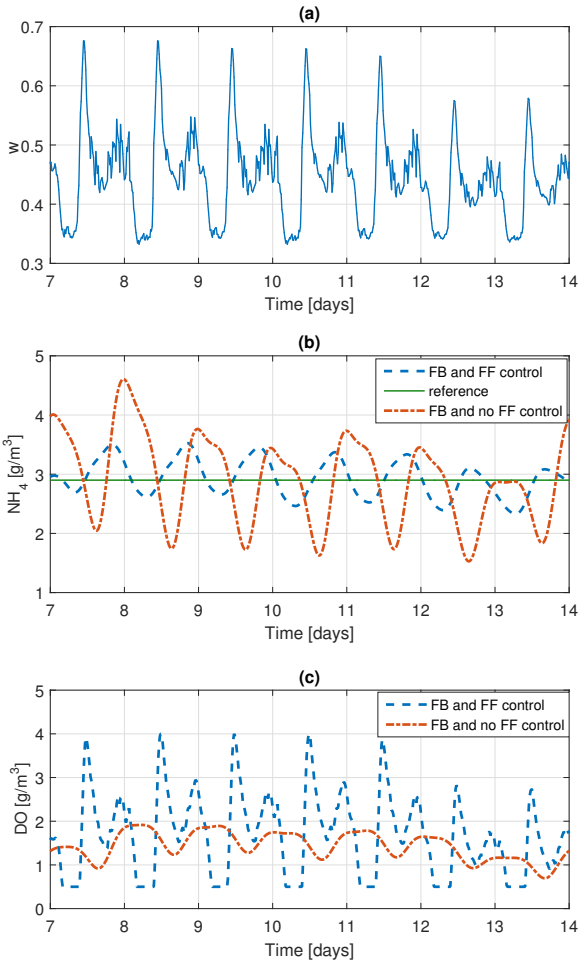

Figure 7: Controller performance in the simplified BSM1 environment: (a) Disturbance signal, (b) NH_4, (c) DO.

Bibliography

[1] Tchobanoglous G., Burton F. L. and Stensel, H.D.: 'Wastewater Engineering: Treatment and Reuse' (Metcalf & Eddy, Inc., New York, NY: McGraw-Hill, 2003)

[2] Gerardi, M. H.: 'Nitrification and Denitrification in the Activated Sludge Process' (New York, NY, USA: Wiley, 2003)

[3] Ingildsen, P.: 'Realising Full-Scale Control in Wastewater Treatment Systems Using In Situ Nutrient Sensors'. Ph.D. thesis, Lund University, Lund, Sweden, 2002

[4] Olsson G., Nielsen M., Yuan, Z., *et al.*: 'Instrumentation, Control and Automation in Wastewater Systems' (London, UK: IWA Publishing, 2005)

[5] Vrečko, D., Hvala, N., Stare, A., *et al.*: 'Improvement of ammonia removal in activated sludge process with feedforward-feedback aeration controllers', Water Sci. Technol., 2006, 53, (4-5), pp.125-132

[6] de Arajo, A. C. B., Gallani, S., Mulas, M., *et al.*: 'Systematic Approach to the Design of Operation and Control Policies in Activated Sludge Systems', Industrial & Engineering Chemistry Research, 2011, 50, (14), pp. 8542-8557

[7] Åmand, L.: 'Ammonium feedback control in wastewater treatment plants'. Ph.D. thesis, Uppsala University, Uppsala, Sweden, 2014

[8] Ingildsen, P., Jeppsson, U. and Olsson, G.: 'Dissolved oxygen controller based on on-line measurements of ammonium combining feed-forward and feedback', Water Sci. Technol., 2002, 45, (4-5), pp. 453-460

[9] Rieger, L., Jones, R. M, Dold, P. and Bott, C. B.: 'Myths About Ammonia Feedforward Aeration Control'. Proc. WEFTEC 2012, New Orleans, LA, USA, September 2012

[10] Rieger, L., Jones, R. M., Dold, P. and Bott, C. B.: 'Ammonia-based feedforward and feedback aeration control in activated sludge processes', Water Environ Res., 2014, 86, (1), pp. 63-73

[11] Chistiakova, T., Carlsson, B. and Wigren, T.: 'Non-linear modeling of the dissolved oxygen to ammonium dynamics in a nitrifying activated sludge process'. Proc. ICA 2017, Quebec City, Quebec, Canada, June 2017, pp. 85-93

[12] Chistiakova, T., Mattsson, P., Carlsson, B. and Wigren, T.: 'Nonlinear system identification of the dissolved oxygen to effluent ammonia dynamics in an activated sludge process'. Proc. IFAC 2017 World Congress, Tolouse, France, July 2017, pp. 3978-3983

[13] Wigren, T.: 'Low-frequency limitations in saturated and delayed networked control'. Proc. IEEE CCA 2015, Manly, Sydney, NSW, Australia, September 2015, pp. 564-571

[14] Wigren, T.: 'Low frequency sensitivity function constraints for nonlinear $\mathcal{L}_2$-stable networked control', Asian J. Contr., 2016, 18, (4), pp. 1200-1218

[15] Chistiakova, T., Wigren, T. and Carlsson, B.: 'Input-Output Stability Design of an Ammonium Based Aeration Controller for Wastewater Treatment'. To appear in Proc. ACC 2018, Milwaukee, USA, June 2018

[16] Sternad, M. and Söderström, T.: 'LQG - optimal feedfoward regulators', Automatica, 1988, 24, (4), pp.557-561

[17] Wigren, T.: 'Wireless feedback and feedforward control subject to rate saturation and uncertain delay', IET Control Theory and Application, 2016, 10, (3), pp. 346-352

[18] Henze, M.: 'Activated sludge model no. 1'. IAWPRC Scientific and Technical Reports, 1, London, UK: IWA Publishing, 1987

[19] Copp, J. B. (ed.): 'The COST Simulation Benchmark - Description and Simulator Manual', Office for Official Publications of the European Communities, , Luxembourg, 2002

[20] Monod, J.: 'The growth of bacterial cultures', Annual Review of Microbiology, 1949, 3, pp. 371-394

[21] Söderström, T. and Stoica, P.: 'System identification' (Hemel Hempstead, UK: Prentice-Hall, 1989)

[22] Glad T. and Ljung, L.: 'Control Theory' (Bodmin, UK: Taylor and Francis, 2000)

[23] Ljung, L.: 'System Identification Toolbox: Users Guide Version 7.4.' (Natick, MA, USA: The Mathworks, 2011)

[24] Vidyasagar, M.: 'Nonlinear Systems Analysis' (Englewood Cliffs, NJ, USA: Prentice-Hall, 1978)

Recent licentiate theses from the Department of Information Technology

2018-001 Kim-Anh Tran: *Static Instruction Scheduling for High Performance on Energy-Efficient Processors*

2017-003 Oscar Samuelsson: *Fault Detection in Water Resource Recovery Facilities*

2017-002 Germán Ceballos: *Modeling the Interactions Between Tasks and the Memory System*

2017-001 Diana Yamalova: *Hybrid Observers for Systems with Intrinsic Pulse-Modulated Feedback*

2016-012 Peter Backeman: *New Techniques for Handling Quantifiers in Boolean and First-Order Logic*

2016-011 Andreas Svensson: *Learning Probabilistic Models of Dynamical Phenomena Using Particle Filters*

2016-010 Aleksandar Zeljić: *Approximations and Abstractions for Reasoning about Machine Arithmetic*

2016-009 Timofey Mukha: *Inflow Generation for Scale-Resolving Simulations of Turbulent Boundary Layers*

2016-008 Simon Sticko: *Towards Higher Order Immersed Finite Elements for the Wave Equation*

2016-007 Volkan Cambazoglou: *Protocol, Mobility and Adversary Models for the Verification of Security*

2016-006 Anton Axelsson: *Context: The Abstract Term for the Concrete*

2016-005 Ida Bodin: *Cognitive Work Analysis in Practice: Adaptation to Project Scope and Industrial Context*

UPPSALA
UNIVERSITET

Department of Information Technology, Uppsala University, Sweden